

- immunoassay for fucosylated fraction of alpha-fetoprotein in patients with hepatocellular carcinoma. *Dig Dis Sci* 2010;55:3576-3583.
20. Villanueva A, Hoshida Y, Toffanin S, Lachenmayer A, Alsinet C, Savić R, et al. New strategies in hepatocellular carcinoma: genomic prognostic markers. *Clin Cancer Res* 2010;16:4688-4694.
  21. Yamashita T, Forgues M, Wang W, Kim JW, Ye Q, Jia H, et al. EpCAM and alpha-fetoprotein expression defines novel prognostic subtypes of hepatocellular carcinoma. *Cancer Res* 2008;68:1451-1461.
  22. Yamashita T, Ji J, Budhu A, Forgues M, Yang W, Wang HY, et al. EpCAM-positive hepatocellular carcinoma cells are tumor-initiating cells with stem/progenitor cell features. *Gastroenterology* 2009;136:1012-1024.
  23. Boyault S, Rickman DS, de Reyniès A, Balabaud C, Rebouissou S, Jeannot E, et al. Transcriptome classification of HCC is related to gene alterations and to new therapeutic targets. *Hepatology* 2007;45:42-52.
  24. Ji J, Shi J, Budhu A, Yu Z, Forgues M, Roessler S, et al. MicroRNA expression, survival, and response to interferon in liver cancer. *N Engl J Med* 2009;361:1437-1447.
  25. Budhu A, Forgues M, Ye QH, Jia HL, He P, Zanetti KA, et al. Prediction of venous metastases, recurrence, and prognosis in hepatocellular carcinoma based on a unique immune response signature of the liver microenvironment. *Cancer Cell* 2006;10:99-111.
  26. Llovet JM, Peña C, Shan M, Lathia C, Bruix J. Biomarkers predicting outcome of patients with advanced hepatocellular carcinoma (HCC) randomized in the phase III SHARP trial. Paper presented at: 59th Annual Meeting of the American Association for the Study of Liver Diseases; October 31-November 4, 2008; San Francisco, CA.
  27. Schwartz M, Dvorchik I, Roayaie S, Fiel MI, Finkelstein S, Marsh JW, et al. Liver transplantation for hepatocellular carcinoma: extension of indications based on molecular markers. *J Hepatol* 2008;49:581-588.
  28. Yang ZF, Ho DW, Ng MN, Lau CK, Yu WC, Ngai P, et al. Significance of CD90+ cancer stem cells in human liver cancer. *Cancer Cell* 2008;13:153-166.
  29. Laurent-Puig P, Legoix P, Bluteau O, Belghiti J, Franco D, Binot F, et al. Genetic alterations associated with hepatocellular carcinomas define distinct pathways of hepatocarcinogenesis. *Gastroenterology* 2001;120:1763-1773.
  30. Korita PV, Wakai T, Shirai Y, Matsuda Y, Sakata J, Cui X, et al. Overexpression of osteopontin independently correlates with vascular invasion and poor prognosis in patients with hepatocellular carcinoma. *Hum Pathol* 2008;39:1777-1783.
  31. Weinstein IB, Joe A. Oncogene addiction. *Cancer Res* 2008;68:3077-3080.
  32. Piccart-Gebhart MJ, Procter M, Leyland-Jones B, Goldhirsch A, Untch M, Smith I, et al.; for Herceptin Adjuvant (HERA) Trial Study Team. Trastuzumab after adjuvant chemotherapy in HER2-positive breast cancer. *New Engl J Med* 2005;353:1659-1672.
  33. Kobayashi S, Boggon TJ, Dayaram T, Jänne PA, Kocher O, Meyerson M, et al. EGFR mutation and resistance of non-small-cell lung cancer to gefitinib. *N Engl J Med* 2005;352:786-792.
  34. Demetri GD, Wang Y, Wehrle E, Racine A, Nikolova Z, Blanke CD, et al. Imatinib plasma levels are correlated with clinical benefit in patients with unresectable/metastatic gastrointestinal stromal tumors. *J Clin Oncol* 2009;27:3141-3147.
  35. Loupakis F, Pollina L, Stasi I, Ruzzo A, Scartozzi M, Santini D, et al. PTEN expression and KRAS mutations on primary tumors and metastases in the prediction of benefit from cetuximab plus irinotecan for patients with metastatic colorectal cancer. *J Clin Oncol* 2009;27:2622-2629.
  36. Flaherty KT, Puzanov I, Kim KB, Ribas A, McArthur GA, Sosman JA, et al. Inhibition of mutated, activated BRAF in metastatic melanoma. *N Engl J Med* 2010;363:809-819.
  37. Féré C, André F, Soria JC. Molecular circuits of solid tumors: prognostic and predictive tools for bedside use. *Nat Rev Clin Oncol* 2010;7:367-380.
  38. Hoshida Y, Toffanin S, Lachenmayer A, Villanueva A, Minguez B, Llovet JM. Molecular classification and novel targets in hepatocellular carcinoma: recent advancements. *Semin Liver Dis* 2010;30:35-51.
  39. Llovet JM, Bruix J. Molecular targeted therapies in hepatocellular carcinoma. *Hepatology* 2008;48:1312-1327.
  40. Llovet JM, Ricci S, Mazzaferro V, Hilgard P, Gane E, Blanc JF, et al.; for SHARP Investigators Study Group. Sorafenib in advanced hepatocellular carcinoma. *N Engl J Med* 2008;359:378-390.
  41. Wilhelm SM, Carter C, Tang L, Wilkie D, McNabola A, Rong H, et al. BAY 43-9006 exhibits broad spectrum oral antitumor activity and targets the RAF/MEK/ERK pathway and receptor tyrosine kinases involved in tumor progression and angiogenesis. *Cancer Res* 2004;64:7099-7109.

# SRPX2 Is a Novel Chondroitin Sulfate Proteoglycan That Is Overexpressed in Gastrointestinal Cancer

Kaoru Tanaka<sup>1,2</sup>, Tokuzo Arao<sup>1</sup>, Daisuke Tamura<sup>1</sup>, Keiichi Aomatsu<sup>1</sup>, Kazuyuki Furuta<sup>1</sup>, Kazuko Matsumoto<sup>1</sup>, Hiroyasu Kaneda<sup>1,2</sup>, Kanae Kudo<sup>1</sup>, Yoshihiko Fujita<sup>1</sup>, Hideharu Kimura<sup>1</sup>, Kazuyoshi Yanagihara<sup>3</sup>, Yasuhide Yamada<sup>4</sup>, Isamu Okamoto<sup>2</sup>, Kazuhiko Nakagawa<sup>2</sup>, Kazuto Nishio<sup>1\*</sup>

**1** Department of Genome Biology, Kinki University School of Medicine, Osaka-Sayama, Osaka, Japan, **2** Department of Medical Oncology, Kinki University School of Medicine, Osaka-Sayama, Osaka, Japan, **3** Department of Life Science, Faculty of Pharmacy, Yasuda Women's University, Asaminami-ku, Hiroshima, Japan, **4** Department of Medical Oncology, National Cancer Center Hospital, Chuo-ku, Tokyo, Japan

## Abstract

SRPX2 (Sushi repeat-containing protein, X-linked 2) has recently emerged as a multifunctional protein that is involved in seizure disorders, angiogenesis and cellular adhesion. Here, we analyzed this protein biochemically. SRPX2 protein was secreted with a highly posttranslational modification. Chondroitinase ABC treatment completely decreased the molecular mass of purified SRPX2 protein to its predicted size, whereas heparitinase, keratanase and hyaluronidase did not. Secreted SRPX2 protein was also detected using an anti-chondroitin sulfate antibody. These results indicate that SRPX2 is a novel chondroitin sulfate proteoglycan (CSPG). Furthermore, a binding assay revealed that hepatocyte growth factor dose-dependently binds to SRPX2 protein, and a ligand-glycosaminoglycans interaction was speculated to be likely in proteoglycans. Regarding its molecular architecture, SRPX2 has sushi repeat modules similar to four other CSPGs/lecticans; however, the molecular architecture of SRPX2 seems to be quite different from that of the lecticans. Taken together, we found that SRPX2 is a novel CSPG that is overexpressed in gastrointestinal cancer cells. Our findings provide key glycobiological insight into SRPX2 in cancer cells and demonstrate that SRPX2 is a new member of the cancer-related proteoglycan family.

**Citation:** Tanaka K, Arao T, Tamura D, Aomatsu K, Furuta K, et al. (2012) SRPX2 Is a Novel Chondroitin Sulfate Proteoglycan That Is Overexpressed in Gastrointestinal Cancer. *PLoS ONE* 7(1): e27922. doi:10.1371/journal.pone.0027922

**Editor:** Hana Algül, Technische Universität München, Germany

**Received:** June 28, 2011; **Accepted:** October 27, 2011; **Published:** January 5, 2012

**Copyright:** © 2012 Tanaka et al. This is an open-access article distributed under the terms of the Creative Commons Attribution License, which permits unrestricted use, distribution, and reproduction in any medium, provided the original author and source are credited.

**Funding:** This work was supported by funds for the Comprehensive 3rd Term of the 10-Year Strategy for Cancer Control, a Grant-in-Aid for Scientific Research from the Ministry of Education, Culture, Sports, Science and Technology of Japan (19209018), and a fund from the Health and Labor Scientific Research Grants. The funders had no role in study design, data collection and analysis, decision to publish, or preparation of the manuscript.

**Competing Interests:** The authors have declared that no competing interests exist.

\* E-mail: knishio@med.kindai.ac.jp

## Introduction

Sushi repeat protein X-linked 2 (SRPX2) was first identified as a gene up-regulated in pro-B leukemia cells and was described as sushi-repeat protein up-regulated in leukemia (SPRUL, [1]). Several years later, SRPX2 was found to be responsible for rolandic seizures associated with oral and speech dyspraxia and mental retardation [2]. The disease-causing mutation (N327S) and a second mutation (Y72S) of SRPX2 were identified, and these mutations resulted in the gain-of-N-glycosylated form of the mutant protein [2]. Although the molecular and biological functions of SRPX2 have been unknown for a long time, a recent study clearly demonstrated that SRPX2 binds to urokinase plasminogen activator receptor (uPAR) in a ligand/receptor interaction and that SRPX2 mutations led to an increase in the SRPX2/uPAR binding affinity [3]. In the vascular endothelial cells, SrpX2 regulates endothelial cell migration and tube formation, and the interaction of SRPX2 and uPAR is also involved in the early phases of endothelial remodeling during angiogenesis [4].

Recently, we demonstrated that SRPX2 is overexpressed in gastric cancer tissue and that expression was associated with a poor clinical outcome [5]. SRPX2 enhances cellular migration and

adhesion in gastric cancer cells and, interestingly, the conditioned-medium obtained from SRPX2-producing cells increased the cellular migration activity and cellular adhesion [5]. We further examined SRPX2, focusing on a biochemical analysis in this study.

## Materials and Methods

### Cell culture

HEK293 was maintained in DMEM medium and SNU-16 and MKN7 were maintained in RPMI1640 medium supplemented with 10% FBS. HUVEC (human umbilical vein endothelial cells) was maintained in Humedia-EG2 (KURABO, Tokyo, Japan) medium with 1% FBS under the addition of EGF and FGF-2. The cells were maintained in a 5% CO<sub>2</sub>-humidified atmosphere at 37°C. These cell lines were obtained from the Japanese Collection of Research Bioresources Collection (Sennan-shi, Osaka).

### Western blotting analysis

The western blotting analysis has been previously described [6]. In brief, cell pellets were lysed in RIPA buffer (Tris-HCl: 50 mM, pH 7.4; NP-40: 1%; Na-deoxycholate: 0.25%; NaCl: 150 mM; EDTA: 1 mM; phenylmethyl-sulfonyl fluoride: 1 mM; aprotinin,

leupeptin, pepstatin: 1 mg/ml each; Na<sub>3</sub>VO<sub>4</sub>: 1 mM; NaF: 1 mM). Cell extracts were electrophoresed on 7.5% (w/v) polyacrylamide gels and transferred to a polyvinylidene di-fluoride membrane (Nihon Millipore, Tokyo, Japan). The membrane was incubated in Tris-buffered saline containing 0.5% Tween 20 with 3% BSA and then reacted with the primary antibodies and the HRP-conjugated secondary antibody for 90 min each. Visualization was achieved with an enhanced chemiluminescent detection reagent (Amersham Biosciences, Buckinghamshire, UK). The following antibodies were used: anti-HA high affinity (Roche Applied Science, Mannheim, Germany), anti-SRPX2 [5] and anti-chondroitin sulfate (CS-56; Seikagaku Kogyo, Tokyo, Japan).

### Detection of endogenous SRPX2 protein

The culture medium was dialyzed against 50 mM of ammonium bicarbonate and lyophilized. The residue was dissolved in 50 mM of Tris-HCl (pH 7.4) and centrifuged at 20,000 rpm for 30 min. The supernatant was filtered through a 0.22- $\mu$ m filter. The filtrate was subjected to fast protein liquid chromatography (FPLC; GE Healthcare UK Ltd. Buckinghamshire, England) separation on HiTrap Q HP columns (5 mL; GE Healthcare). The columns were equilibrated with 50 mM of Tris-HCl (pH 7.4). The samples were then injected onto the columns, which were washed with the same buffer and eluted at a flow rate of 4 mL/min using a linear gradient consisting of 0–2 M NaCl in 50 mM Tris-HCl (pH 7.4) over 45 min. The SRPX2 protein-containing fractions were then performed using gel-filtration chromatography (Superdex200 column, 16 mm $\times$ 60 mm; GE Healthcare).

### Expression constructs and purification of SRPX2-HA/His protein

The method for producing the expression constructs was previously described [5]. Empty and SRPX2-HA/His vectors were then transfected into HEK293 cells using FuGENE6 transfection reagent (Roche Diagnostics, Basel, Switzerland), and the cells were then selected with hygromycin. The stable transfectant HEK293 cells were designated as HEK293-Mock and HEK293-SRPX2-HA/His. The conditioned medium of the HEK293-Mock and HEK293-SRPX2-HA/His cells was subjected to FPLC loading at 3 mL/min on a 5-mL HisTrap HP column (GE Healthcare). The bound protein was washed with 15 mL of wash buffer (WB: 50 mM Na<sub>2</sub>HPO<sub>4</sub>, 10 mM Tris-HCl, 20 mM imidazole [pH 8.0] and 600 mM NaCl) and eluted in elution buffer (EB: WB+230 mM imidazole). The SRPX2-HA/His protein-containing fractions were applied to an FPLC Superdex200 column (16 mm $\times$ 60 mm; GE Healthcare) equilibrated with 0.15 M of ammonium bicarbonate. Elution was carried out using the same buffer at a flow rate of 1 mL/min. The SRPX2-HA/His-containing fractions were verified using western blotting and lyophilized.

### Digestion of SRPX2 by specific GAG-degrading enzymes

Purified SRPX2-HA/His protein was digested with several specific enzymes including chondroitinase ABC and chondroitinase AC II (0.1 units in 40 mM Tris-HCl, 40 mM sodium acetate [pH 8.0] at 37°C for 2 h), chondroitinase B (0.02 units in 20 mM Tris-HCl, 0.25  $\mu$ M calcium acetate [pH 7.5] at 37°C for 2 h), heparinase I and heparinase II (0.05 units in 5 mM calcium acetate, 50 mM sodium acetate [pH 7.0] 37°C for h), keratanase (0.1 units in 7.5  $\mu$ M Tris-HCl [pH 7.4] at 37°C for 2 h), and hyaluronidase (0.02 M acetate buffer, 0.15 M NaCl [pH 6.0] at 60°C for 2 h). Enzymes were purchased from Seikagaku Kogyo. The samples were then analyzed using western blotting.

### Binding Assays

An IAsys resonant mirror biosensor (Affinity Sensors, Cambridge, UK) with a carboxymethyl dextran-sensing cuvette was used to determine the kinetic constants of hepatocyte growth factor (HGF) binding to immobilized SRPX2-HA/His. SRPX2-HA/His was dissolved in 10 mM sodium formate (pH 4.0) and immobilized on the carboxymethyl dextran surface of the cuvette, according to the manufacturer's instructions. Binding experiments were performed in PBS. Changes in the resonant angle were monitored at 1-s intervals for approximately 600 s. Experiments were performed at 25°C with a stirrer speed of 80 rpm. The binding parameters were calculated from the association and dissociation phases of the binding reactions using the non-linear curve fitting FastFit (Affinity Sensors). Bovine serum albumin (BSA) was used as a control.

### Microarray data

The clinical samples of the paired colorectal cancers (CRCs), microarray procedure and analysis method have been previously described [7]. This study was approved by the institutional review board, and written informed consent was obtained from all the patients. All microarray data has been deposited to Center for Information Biology gene Expression database (CIBEX, <http://cibex.nig.ac.jp/index.jsp>) as accession number #CBX205. All data is MIAME compliant and that the raw data has been deposited in a MIAME compliant database (CIBEX), as detailed on the MGED Society website <http://www.mged.org/Workgroups/MIAME/miame.html>.

### Patients and samples

The 30 CRC and 10 paired non-cancerous colonic mucosa samples were analyzed using real-time RT-PCR. The RNA extraction method and the quality check protocol have been previously described [7]. This study was approved by the institutional review board of the National Cancer Center Hospital, and written informed consent was obtained from all the patients.

### Real-time reverse transcription PCR and western blot analysis

The methods used in this section have been previously described [5].

## Results

### Overexpression of SRPX2 in CRC tissues

We evaluated the mRNA expression of *SRPX2* in clinical samples of CRCs in addition to its homologue *SRPX* (*SRPX1*) using microarray data. *SRPX2* expression was markedly up-regulated (20.5 fold,  $p=0.00014$ ) in cancer tissues, compared with paired noncancerous mucosa samples, whereas the putative tumor suppressor gene *SRPX* was down-regulated (0.7 fold,  $p=0.029$ ) in cancer (Fig. 1). The result indicates that *SRPX2* is overexpressed in CRC during carcinogenesis and tumor progression, unlike *SRPX*. Real-time RT-PCR for the 30 CRC and 10 paired non-cancerous colonic mucosa samples confirmed that *SRPX2* mRNA was markedly overexpressed in the CRC samples but was only expressed at a very low level in non-cancerous colonic mucosa (Figure 1B).

### Secreted SRPX2 protein is suspected to be modified posttranslationally

The predicted molecular mass of SRPX2 protein was 53 kDa; however, western blotting revealed that the molecular mass of the secreted SRPX2 protein was highly increased, with smeared bands at an apparent molecular mass of 100–150 kDa in SNU-16 and

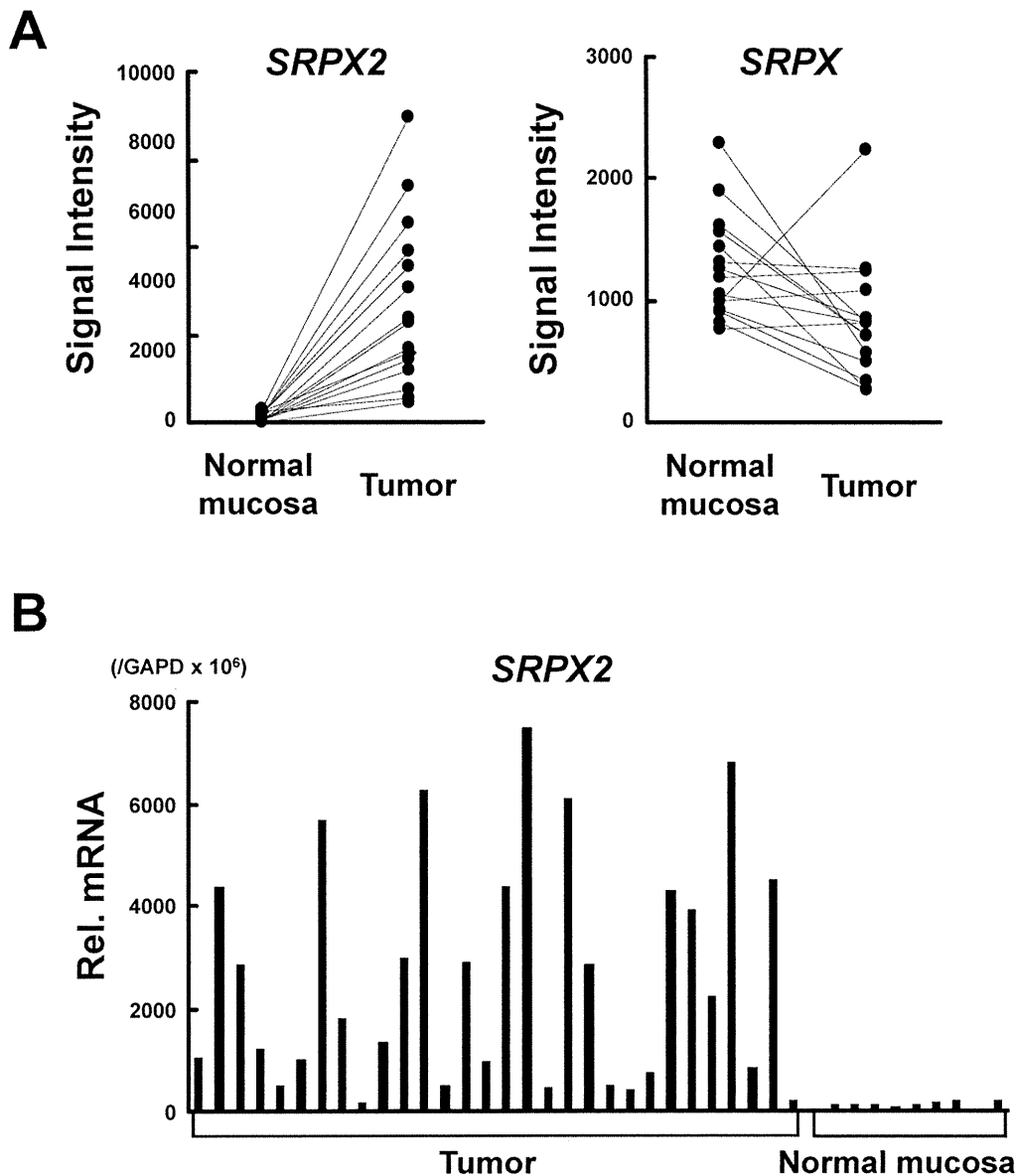


**Figure 1. SRPX2 is overexpressed in colorectal cancer (CRC).** (A) The mRNA expression of *SRPX2* and its homologue *SRPX* in 15 CRC and paired normal colonic mucosa specimens. The values indicate the normalized signal intensity obtained from the microarray data. (B) mRNA expression levels of *SRPX2* determined using real-time RT-PCR. CRC: colorectal cancer, Rel mRNA: normalized mRNA expression levels ( $SRPX2/GAPD \times 10^6$ ). doi:10.1371/journal.pone.0027922.g001

MKN7 cell lines (Fig. 2A). Next, we evaluated the exogenously expressed SRPX2 protein derived from HEK293-Mock and HEK293-SRPX2-HA/His cells. The molecular mass of intracellular SRPX2 protein was similar to the predicted size, while the molecular mass of the secreted-SRPX2 protein was highly increased (100–150 kDa). Smear bands were also detected using both anti-HA and anti-SRPX2 antibodies (Fig. 2B). The non-smear bands at 120 kDa in cell lysate are endogenous SRPX2. These results suggested that secreted SRPX2 protein may undergo posttranslational modifications.

#### SRPX2 is a novel chondroitin sulfate proteoglycan

Based on the appearance of the smeared bands at a highly increased molecular mass, we hypothesized that SRPX2 is a proteoglycan with glycosaminoglycan (GAG) chains. Accordingly, we treated purified-SRPX2 protein obtained from the cultured

medium of HEK293-Mock (empty control) or HEK293-SRPX2-HA/His cells with chondroitinase ABC, heparitinase 1, heparitinase 2, keratanase, chondroitinase AcII, chondroitinase B, and hyaluronidase. Western blotting revealed that the molecular mass of the secreted SRPX2 protein was clearly decreased by chondroitinase ABC digestion, but not by heparitinase or keratanase or hyaluronidase (Fig. 3A, 3B). Further chondroitinase treatment showed that chondroitinase ABC and chondroitinase AcII completely digested GAGs on SRPX2, but that chondroitinase B partially digested these chains (Fig. 3B). A small digested SRPX2 protein was also detected using anti-SRPX2 antibody (Fig. 3C, 3D). These results indicate that SRPX2 contains chondroitin sulfate GAG chains and is a novel chondroitin sulfate proteoglycan (CSPG). In addition, the partial digestion by chondroitinase B suggests that a dermatan sulfate component may be included in the chondroitin sulfate GAG chains. Next, we

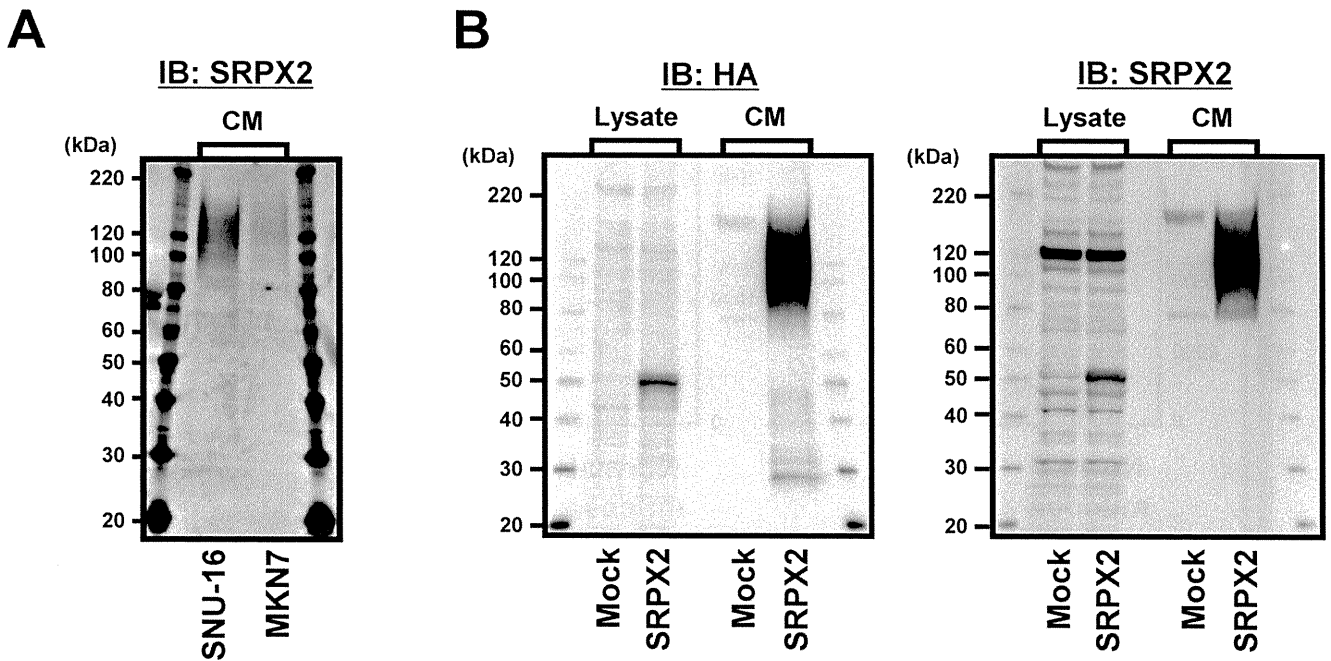


**Figure 2. Secreted SRPX2 protein is suspected to be modified posttranslationally.** (A) Secreted form of endogenous SRPX2 protein obtained from culture medium (CM) in SNU-16 and MKN7 cells. CM was subjected to ion exchange chromatography and used for western blotting analysis using anti-SRPX2 antibody. (B) Western blotting for exogenous SRPX2 protein obtained from cell lysate and CM using anti-SRPX2 and anti-HA antibody. Stable transfectant HEK293 cells, introducing the full-length cDNA fragment encoding human SRPX2 with HA and the His-tag vector or empty vector, were used for analysis. The non-smear bands at 120 kDa in cell lysate are endogenous SRPX2. Mock: HEK293-Mock cells, SRPX2: HEK293-SRPX2-HA/His cells. IB: immunoblotting, Lysate: cell lysate, CM: culture medium.  
doi:10.1371/journal.pone.0027922.g002

confirmed the results of enzymatic digestion against endogenous SRPX2 from HUVEC using western blotting with anti-SRPX2 antibody and a similar result was obtained (Fig. 4A). Anti-chondroitin sulfate antibody (CS-56) also detected the chondroitin sulfate GAG on SRPX2 (Fig. 4B). The non-smear bands at 120 kDa in cell lysate are endogenous SRPX2.

#### HGF binds to SRPX2

It is well known that several ligands including HGF, heparin-binding EGF-like growth factor, fibroblast growth factor 2 and vascular endothelial growth factor are capable of binding to the GAG chain and that such interactions are considered to be a unique characteristic of GAGs and proteoglycans [8]. According to a report on CSPG endocan and HGF binding [9], we examined the interaction between HGF and GAGs using an IAsys resonant mirror biosensor. HGF dose-dependently bound to the GAGs of SRPX2, while control BSA did not (Fig. 5A). The  $K_d$  value of this interaction, calculated from the ratio of  $K_{diss}/K_{ass}$ , was 5.6 nM; these data were similar to those for previously reported data on HGF and endocan [9]. Next, we examined the biological function of SRPX2 on HGF. HGF increased the proliferation of HUVECs, and the addition of purified SRPX2 protein into the medium significantly increased HGF-induced proliferation (Figure 5B). These results suggest that the interaction of HGF with SRPX2 has a positive effect on angiogenesis.

#### SRPX2 has unique molecular architectures compared with other sushi repeat module-containing CSPG

Data from publicly available databases (<http://smart.embl-heidelberg.de/>) and a previous report [10] showed that SRPX2 has three sushi repeat modules (also known as complement control

protein modules or short consensus repeats) and one hyaline domain (Fig. 6). Interestingly, four CSPG (agrecan, versican, neurocan and brevican; also known as lecticans) are present among the sushi repeat module-containing family, and their common molecular architectures consist of one immunoglobulin-like domain, 2~4 LINK domains, one EGF-like domain, one C-type lectin, and one sushi repeat module (Fig. 6). The presence of a sushi repeat module and classification as a CSPG are the same for SRPX2 and lecticans, but the other molecular architectures of SRPX2 are quite different.

Taken together, these findings indicate that SRPX2 is a novel CSPG that is overexpressed in gastrointestinal cancer cells.

#### Discussion

The extensive use and structural diversity of sushi repeat modules presumably reflects the versatility of a structural scaffold that has been adapted by evolution to suit many purposes, both architectural and functional, such as the mediation of specific protein-protein and protein-carbohydrate interactions [10–12]. Meanwhile, SRPX2 has one hyaline domain, which appears to be involved in cellular adhesion. Hyaline domains have been identified in several eukaryotic proteins and are often associated with sushi repeat modules or arranged in multiple copies [13]. These characteristics of the molecular architectures of SRPX2, based on knowledge of protein-protein interactions, may contribute to ligand/receptor interactions between SRPX2 and uPAR, with implications for disorders of the language cortex, cognition, and angiogenesis [3,4].

We have demonstrated that SRPX2 is a novel CSPG, suggesting that SRPX2 may have additional as yet unknown biological functions as a proteoglycan, including interactions with

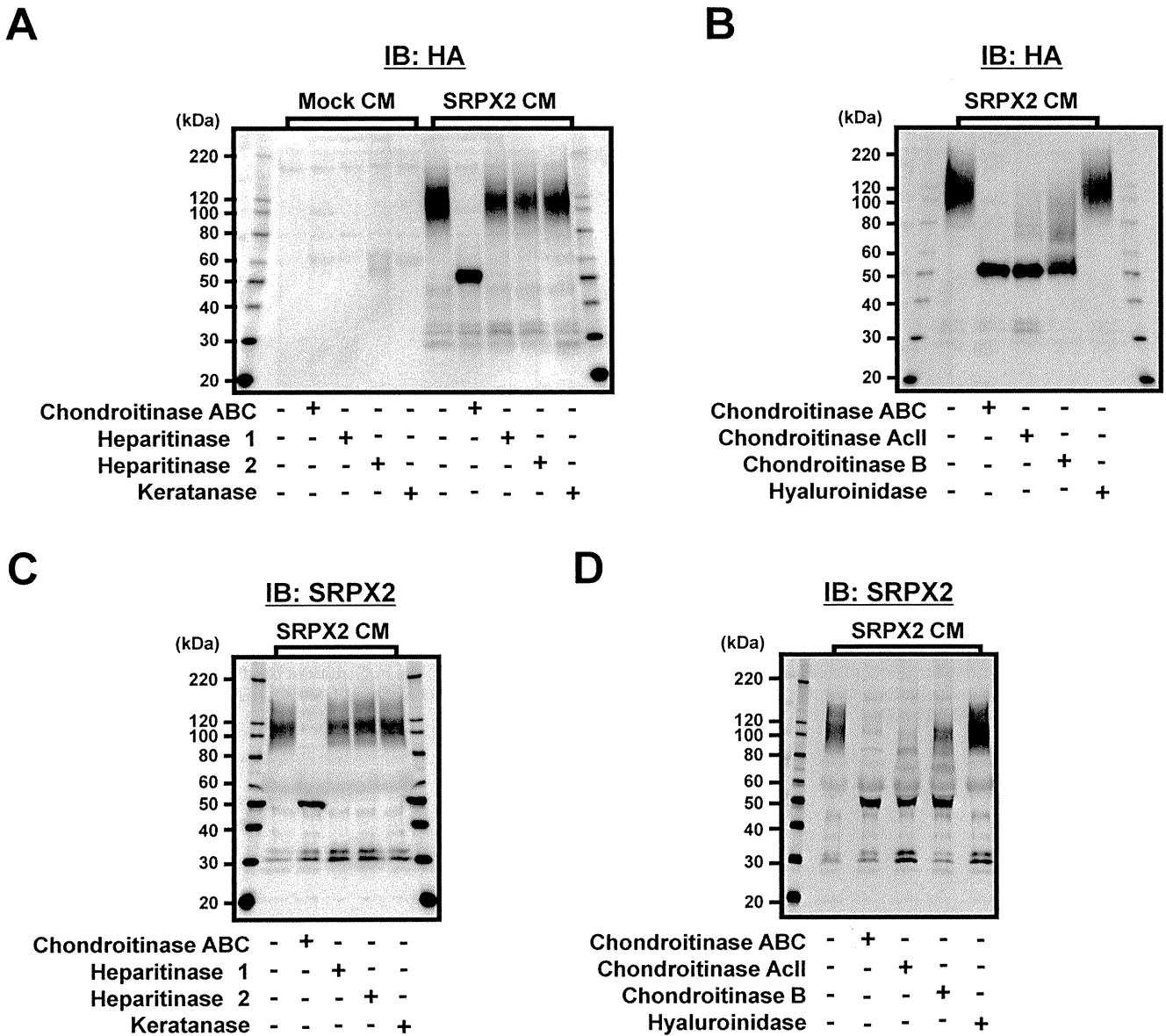


**Figure 3. Effects of chondroitinases on SRPX2.** (A, B) Purified SRPX2 protein obtained from cultured medium of HEK293-Mock or HEK293-SRPX2-HA/His cells were digested with chondroitinase ABC, heparitinase 1, heparitinase 2, keratanase, chondroitinase AclI, chondroitinase B and hyaluroinidase. The effect of digestion of the glycosaminoglycan chains was detected using western blotting using anti-HA (A, B) and anti-SRPX2 (C, D) antibody. IB: immunoblotting, CM: culture medium. Mock: HEK293-Mock cells, SRPX2: HEK293-SRPX2-HA/His cells.  
doi:10.1371/journal.pone.0027922.g003

various extracellular signaling molecules such as growth factors, morphogens, enzymes and chemokines and/or may act at the cell-extracellular-matrix interface to modulate cell signaling. The conditioned-medium of SRPX2-producing cells markedly enhanced cellular adhesion in various cancer cell lines [5]; this result can be explained by the biological function of SRPX2 as a proteoglycan. In addition, although we have only demonstrated that HGF can bind to SRPX2, our results suggest that other known GAG-interacting ligands may be capable of binding to the GAG chain of SRPX2. Therefore, the function of ligand-SRPX2 binding may widely affect the activities of signaling pathway critical to cancer cells, including cellular proliferation, apoptosis, migration and survival [14]. In addition, SRPX2 was found to be secreted and may act as an extracellular matrix protein similar to other

proteoglycans; indeed coating the culture dish with SRPX2 protein markedly enhanced cellular adhesion [5], supporting this idea.

Vascular endothelial cells HUVEC markedly express SRPX2 to the same extent as high-expressing cancer cell lines [5]. A recent report demonstrated that SrpX2 is a novel mediator of angiogenesis and a key molecule involved in the invasive migration of angiogenic endothelium through its role as a ligand for vascular uPAR [4]. Our findings also support the involvement of SRPX2 in angiogenesis from another aspect of proteoglycans. Since endocan is well-known as a vascular endothelial cells-specific CSPG [8], SRPX2 may be categorized as a vascular-related CSPG similar to endocan.

In conclusion, we found that SRPX2 is a novel chondroitin sulfate proteoglycan that is overexpressed in gastrointestinal

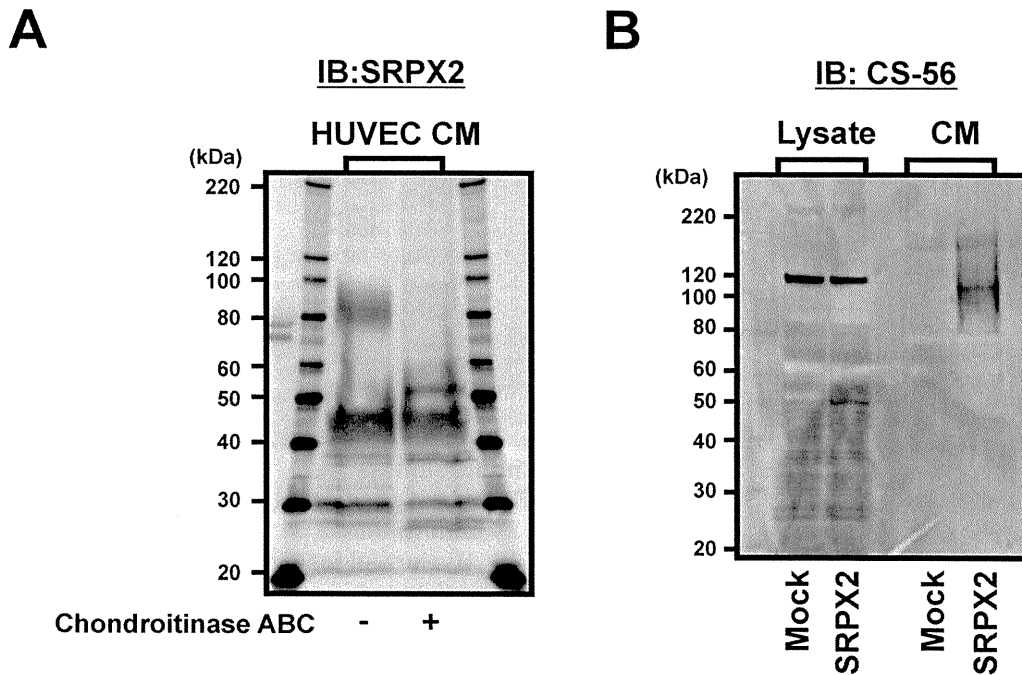


**Figure 4. Detection of chondroitin sulfate glycosaminoglycan and binding of HGF to SRPX2.** (A) Chondroitinase ABC digestion for endogenous SRPX2 protein derived from HUVEC (human umbilical vein endothelial cells). The SRPX2 protein was detected using anti-SRPX2 antibody. (B) Western blotting for SRPX2 protein using anti-chondroitin sulfate antibody (CS-56). The non-smear bands at 120 kDa in cell lysate are endogenous SRPX2. IB: immunoblotting, Lysate: cell lysate, CM: culture medium. Mock: HEK293-Mock cells, SRPX2: HEK293-SRPX2-HA/His cells. doi:10.1371/journal.pone.0027922.g004

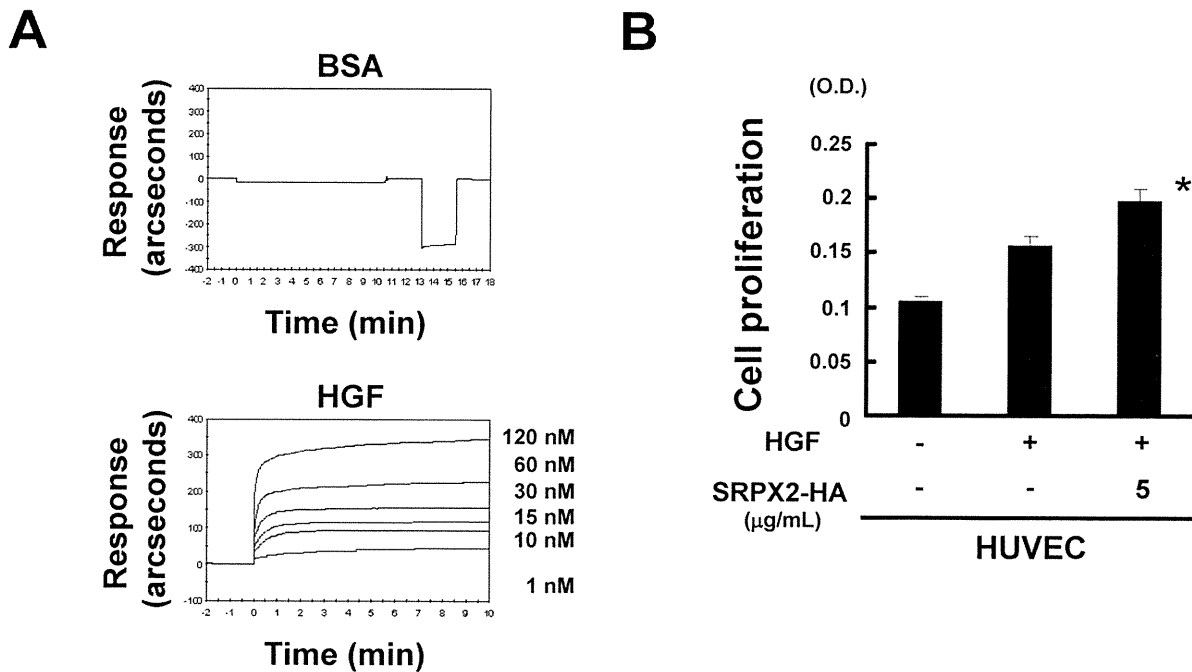


**Figure 5. Binding of HGF to SRPX2 at the indicated concentrations.** (A) IAsys resonant mirror biosensor was used for analysis. Bovine serum albumin (BSA) was used as a negative control. (B) Cell proliferation of HUVECs evaluated using an MTT assay. The HUVECs were stimulated with or without 10 ng/mL of HGF and 5 µg/mL of purified SRPX2 protein for 72 hours. \*, SRPX2 (-) vs. (+),  $p < 0.05$ . doi:10.1371/journal.pone.0027922.g005

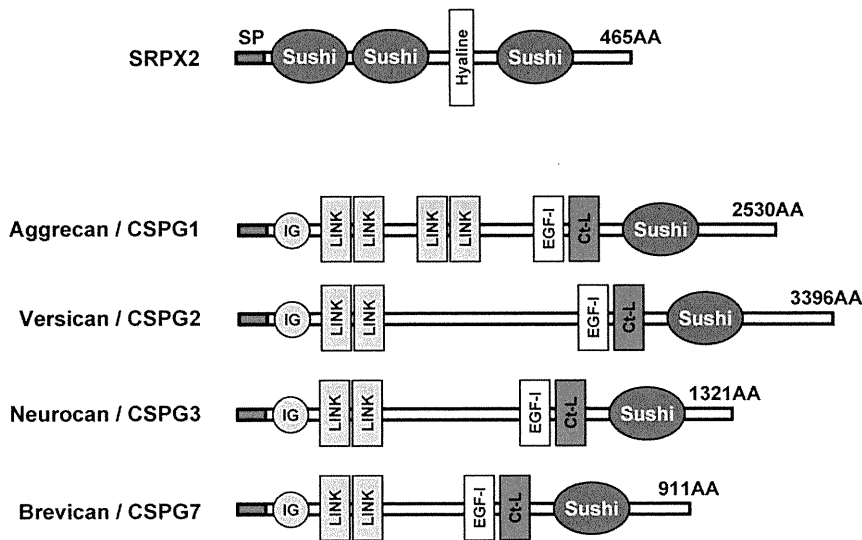


**Figure 6. Molecular architectures of SRPX2.** The data was obtained from the public database SMART (<http://smart.embl-heidelberg.de/>). SRPX2 has three sushi repeat modules and one hyaline domain. Four sushi repeat module-containing CSPG (aggrecan, versican, neurocan and brevican; also known as lecticans) are also shown. SP: signal peptides, AA: amino acids. Sushi: sushi repeat modules/CCP/short consensus repeats, Hyaline: hyaline domain, IG: immunoglobulin-like, LINK: hyaluronan-binding, EGF-I: EGF-like ( $\text{Ca}^{2+}$ -binding), Ct-L: C-type lectin.  
doi:10.1371/journal.pone.0027922.g006

cancer. Our findings provide key glyco-biological knowledge of this protein in cancer cells.

## Acknowledgments

We thank Mrs. Eiko Honda (Life Science Center, Kinki University School of Medicine) for her technical assistance and Mr. Kiyotaka Okada (Department of Physiology, Kinki University School of Medicine) for technical advice.

## References

- Kurosawa H, Goi K, Inukai T, Inaba T, Chang KS, et al. (1999) Two candidate downstream target genes for E2A-HLF. *Blood* 93: 321–32.
- Roll P, Rudolf G, Pereira S, Royer B, Scheffer IE, et al. (2006) SRPX2 mutations in disorders of language cortex and cognition. *Hum Mol Genet* 15: 1195–207.
- Royer-Zemmour B, Ponsolle-Lenfant M, Gara H, Roll P, Lévêque C, et al. (2008) Epileptic and developmental disorders of the speech cortex: ligand/receptor interaction of wild-type and mutant SRPX2 with the plasminogen activator receptor uPAR. *Hum Mol Genet* 17: 3617–30.
- Miljkovic-Licina M, Hammel P, Garrido-Urbani S, Bradfield PF, Szeptowski P, et al. (2009) Sushi repeat protein X-linked 2, a novel mediator of angiogenesis. *FASEB J* 23: 4105–16.
- Tanaka K, Arai T, Maegawa M, Matsumoto K, Kaneda H, et al. (2009) SRPX2 is overexpressed in gastric cancer and promotes cellular migration and adhesion. *Int J Cancer* 124: 1072–80.
- Matsumoto K, Arai T, Tanaka K, Kaneda H, Kudo K, et al. (2009) mTOR signal and hypoxia-inducible factor-1 alpha regulate CD133 expression in cancer cells. *Cancer Res* 69: 7160–4.
- Kaneda H, Arai T, Tanaka K, Tamura D, Aomatsu K, et al. (2010) FOXQ1 is overexpressed in colorectal cancer and enhances tumorigenicity and tumor growth. *Cancer Res* 70: 2053–63.
- Yamada S, Sugahara K (2008) Potential therapeutic application of chondroitin sulfate/dermatan sulfate. *Curr Drug Discov Technol* 5: 289–301.
- Bécharde D, Gentina T, Delehedde M, Scherpereel A, Lyon M, et al. (2001) Endocan is a novel chondroitin sulfate/dermatan sulfate proteoglycan that promotes hepatocyte growth factor/scatter factor mitogenic activity. *J Biol Chem* 276: 48341–9.
- Soares DC, Gerloff DL, Syme NR, Coulson AF, Parkinson J, et al. (2005) Large-scale modelling as a route to multiple surface comparisons of the CCP module family. *Protein Eng Des Sel* 18: 379–88.
- Kirkitadze MD, Barlow PN (2001) Structure and flexibility of the multiple domain proteins that regulate complement activation. *Immunol Rev* 180: 146–61.
- O’Leary JM, Bromek K, Black GM, Uhrinova S, Schmitz C, et al. (2004) Backbone dynamics of complement control protein (CCP) modules reveals mobility in binding surfaces. *Protein Sci* 13: 1238–50.
- Callebaut I, Gilgès D, Vigon I, Morion JP (2000) HYR, an extracellular module involved in cellular adhesion and related to the immunoglobulin-like fold. *Protein Sci* 9: 1382–90.
- Sasisekharan R, Shriver Z, Venkataraman G, Narayanasami U (2002) Roles of heparan-sulphate glycosaminoglycans in cancer. *Nat Rev Cancer* 2: 521–8.

## Author Contributions

Conceived and designed the experiments: TA K. Nakagawa K. Nishio. Performed the experiments: KT DT KA KF KM H. Kaneda KK KY YF. Analyzed the data: TA H. Kimura KY IO. Contributed reagents/materials/analysis tools: YY. Wrote the paper: KT TA K. Nishio.

## A phase I/II trial of the oral antiangiogenic agent TSU-68 in patients with advanced hepatocellular carcinoma

Fumihiko Kanai · Haruhiko Yoshida · Ryosuke Tateishi · Shinpei Sato · Takao Kawabe · Shuntaro Obi · Yuji Kondo · Makoto Taniguchi · Kazumi Tagawa · Masafumi Ikeda · Chigusa Morizane · Takuji Okusaka · Hitoshi Arioka · Shuichiro Shiina · Masao Omata

Received: 26 December 2009 / Accepted: 28 March 2010 / Published online: 14 April 2010  
© Springer-Verlag 2010

### Abstract

**Purpose** We studied the safety and effectiveness of TSU-68, an oral tyrosine kinase inhibitor of vascular endothelial growth factor receptor-2, platelet-derived growth factor receptor and fibroblast growth factor receptor, in patients with advanced hepatocellular carcinoma (HCC).

**Methods** Patients with unresectable or metastatic HCC were eligible for enrollment. In phase I, the safety, tolerability and pharmacokinetics were assessed in patients

stratified based on liver function, from no cirrhosis to Child–Pugh class B. The safety and effectiveness were assessed in phase II at the dose determined in phase I.

**Results** Twelve patients were enrolled in phase I. Dose-limiting toxicities were found with TSU-68 at the dose of 400 mg bid in Child–Pugh B patients, and 200 mg bid was established as the phase II dose. Phase II included 23 additional patients, and the safety and efficacy were evaluated in a total of 35 patients. One patient (2.9%) had a complete response. Two patients (5.7%) had a partial response, and 15 patients (42.8%) showed a stable disease. The median time to progression was 2.1 months, and the median overall survival was 13.1 months. Common adverse events were hypoalbuminemia, diarrhea, anorexia, abdominal pain, malaise, edema and AST/ALT elevation. The analysis of angiogenesis-related parameters suggests that serum-soluble vascular cell adhesion molecule-1 is a possible marker to show the response.

**Conclusions** TSU-68 at a dose of 200 mg bid determined by stratification into liver function, showed promising preliminary efficacy with a high safety profile in patients with HCC who had been heavily pre-treated.

**Keywords** Advanced HCC · Liver function · TSU-68 · Pharmacokinetics · Tolerability · Angiogenesis

F. Kanai · H. Yoshida · R. Tateishi · S. Sato · T. Kawabe · S. Shiina · M. Omata  
Department of Gastroenterology, University of Tokyo, Tokyo, Japan

F. Kanai  
Department of Clinical Drug Evaluation,  
Graduate School of Medicine, University of Tokyo,  
Tokyo, Japan

S. Obi  
Department of Hepatology, Kyoundo Hospital, Tokyo, Japan

Y. Kondo · M. Taniguchi · K. Tagawa  
Department of Gastroenterology, Mitsui Memorial Hospital,  
Tokyo, Japan

M. Ikeda · C. Morizane · T. Okusaka  
Hepatobiliary and Pancreatic Oncology Division,  
National Cancer Center Hospital, Tokyo, Japan

H. Arioka  
Division of Medical Oncology, Yokohama Rosai Hospital,  
Yokohama, Japan

F. Kanai (✉)  
Department of Gastroenterology, Chiba University Hospital,  
1-8-1 Inohana, Chuo-ku, Chiba 260-8677, Japan  
e-mail: kanaif@faculty.chiba-u.jp

### Introduction

Hepatocellular carcinoma (HCC) is the fifth most common malignancy worldwide, with ~626,000 new cases reported annually [1]. Potentially curative treatments such as surgical therapy (resection and liver transplantation) and locoregional procedures (radiofrequency ablation) are indicated in early stage HCC. However, disease that is

diagnosed at an advanced stage or with progression after locoregional therapy has a dismal prognosis owing to the underlying liver disease [2]. Although no systemic therapy was effective for advanced HCC, two randomized, placebo-controlled studies have proven the survival benefits of sorafenib in such patients [3, 4].

TSU-68 is an orally administered, small-molecule, multiple receptor tyrosine kinase inhibitor that targets vascular endothelial growth factor receptor-2 (VEGFR-2), platelet-derived growth factor receptor (PDGFR) and fibroblast growth factor receptor (FGFR) [5–9]. As HCC is a highly vascular tumor, several antiangiogenic agents have been tested for the treatment of HCC [3, 4]. Since it is a potent antiangiogenic agent, TSU-68 is also expected to be effective against HCC. However, most patients with HCC have accompanying liver cirrhosis or hepatitis. Therefore, its safety must be reevaluated in the presence of liver function impairment [10, 11]. In particular, concerns have been expressed about impairment of the pharmacokinetics of TSU-68, which is eliminated predominantly through hepatic metabolism, oxidation and glucuronidation [12, 13].

From three phase I studies that have been conducted in Japan on patients with solid tumors, the administration of TSU-68 twice daily after meals was selected as the recommended dose regimen [14, 15]. In this regimen, although no dose-limiting toxicity (DLT) exists at dose levels of 200–500 mg/m<sup>2</sup>/dose, the higher dose showed some unacceptable adverse events for an antitumor drug that is administered for long-term consecutive treatment. No obvious dose-dependent increases were detected in the maximum concentration ( $C_{max}$ ) or the area under the curve ( $AUC_{0-t}$ ) over the dose range, which was probably due to a saturation of absorption. Consequently, a dose of 400 mg/dose bid was determined to be the recommended dosage of TSU-68 [14, 15].

In the phase I step of our trial, the safety, tolerance and pharmacokinetics (PK) of TSU-68 at the recommended dose were assessed in successive cohorts of patients with various degrees of liver function: no cirrhosis, Child–Pugh class A and Child–Pugh class B cirrhosis, allowing for dose reduction when necessary. In phase II, we evaluated the effectiveness of TSU-68 against advanced HCC.

## Patients and methods

### Eligibility criteria

The eligibility criteria were histologically confirmed HCC; no indication for or no response to resection, ablation or transcatheter arterial chemoembolization (TACE); age

20–74 years old; World Health Organization performance status of  $\leq 2$ ; life expectancy of  $\geq 90$  days; and white blood cells  $\geq 3,000/\mu\text{l}$  or neutrophils  $\geq 1,500/\mu\text{l}$ ; hemoglobin  $\geq 8.0$  g/dl; platelets  $\geq 75,000/\mu\text{l}$ ; liver function Child–Pugh A or B; total bilirubin  $\leq 2.5$  mg/dl; AST and ALT  $\leq 200$  U/l; albumin  $\geq 3$  g/dl; prothrombin time [%]  $\geq 40$  and serum creatinine  $\leq 1.5$  mg/dl. The criteria for patients in Level 1 of phase I were platelets  $\geq 130,000/\mu\text{l}$ , AST and ALT  $\leq 100$  U/l; total bilirubin below or equal to the upper limit of normal and albumin equal to or over the lower limit of normal.

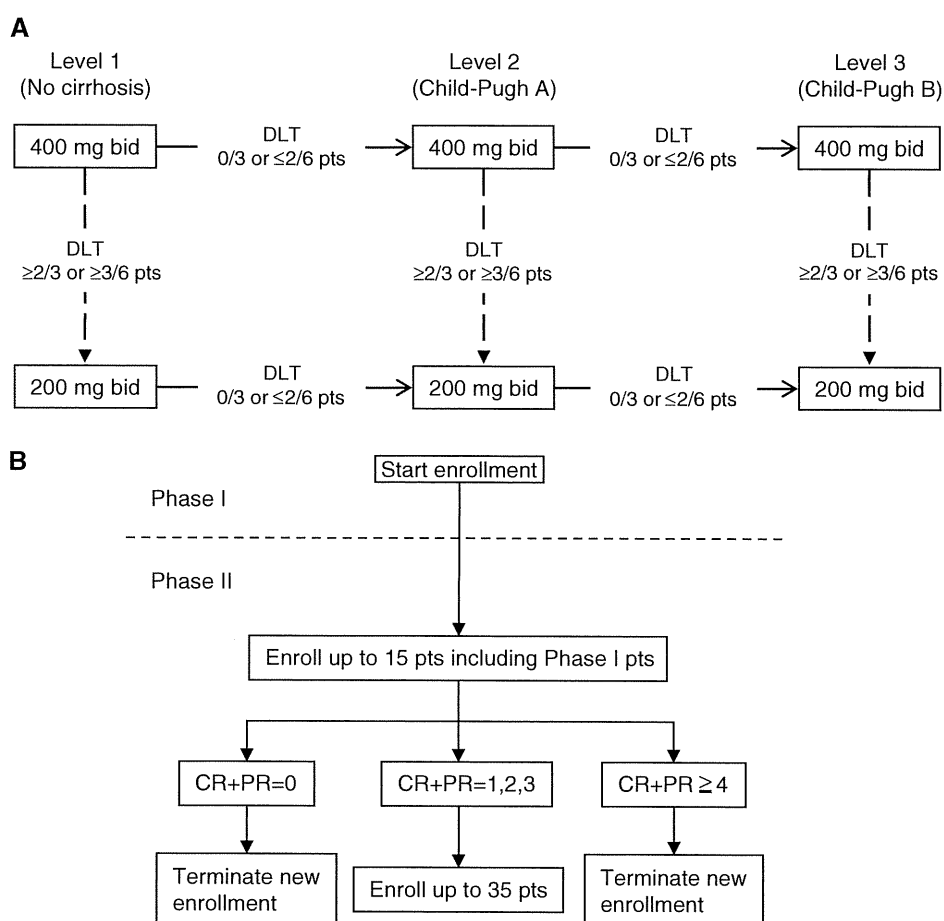
Patients were not eligible if they had received ablation, TACE, chemotherapy or radiotherapy within 4 weeks or surgery within 6 weeks. Patients were excluded if they had clinical evidence of central nervous system metastasis, severe cardiovascular disorders, hepatic encephalopathy, uncontrollable pleural effusion or ascites or a serious infection. Patients who needed prophylactic variceal ligation or sclerotherapy were excluded.

All patients were informed of the purpose and methods of the study and provided written informed consent in accordance with national and institutional guidelines. The study was approved by the institutional review board at each of the three participating hospitals and was performed in accordance with the Declaration of Helsinki and Good Clinical Practice Guidelines.

### Study design and treatment

This was an open-label phase I/II study. In phase I, eligible patients were stratified into three groups based on hepatic function: Level 1, no cirrhosis; Level 2, Child–Pugh class A; and Level 3, Child–Pugh class B. The safety, tolerability and PK were evaluated in each successive cohort. DLT was defined as grade 3 or 4 non-hematological toxicity or grade 4 hematological toxicity according to the National Cancer Institute Common Toxicity Criteria (NCI-CTC) version 2. As shown in Fig. 1a, the dosage of 400 mg bid was first assessed in three patients at Level 1, each treated for one cycle (28 days). If no DLT was observed, three patients at Level 2 were treated with the same dosage. However, if one patient developed DLT, another three patients at Level 1 were added, based on a 3 + 3 study design [16]. If DLT was observed in no more than two of the six patients, three patients at Level 2 were enrolled. By contrast, if more than one of the first three patients or more than two of the six patients developed DLT, the other three patients at Level 1 were treated with half the dosage. The level transition and dose reduction were planned similarly. Drug administration was continued until no evidence of disease progression was observed, unacceptable drug-related toxicity occurred or the patient withdrew consent.

**Fig. 1** TSU-68 phase I/II study schema. **a** In phase I, patients were stratified into three groups based on hepatic function, and the toxicity and pharmacokinetics were assessed from Level 1 (no cirrhosis) to Level 3 (Child–Pugh B) by enrolling three patients at each level. *Bid* twice daily, *DLT* dose-limiting toxicity, *pts* patients. **b** Patient enrollment procedure based on the two-step method of Fleming [17]



Patients were accrued using Fleming's optimal two-stage method [17], allowing for an interim evaluation that would be performed when 15 patients (including phase I) were enrolled (Fig. 1b). TSU-68 would be judged "effective" if efficacy (complete or partial response) was observed in four or more patients and "ineffective" if efficacy was observed in none. If efficacy were confirmed in one to three patients, phase II would be performed at the dosage determined in phase I using 20 additional patients (35 patients in total).

#### Drug administration

TSU-68 (*Z*)-3-[2,4-dimethyl-5-(2-oxo-1,2-dihydro-indol-3-ylidenemethyl)-1H-pyrrol-3-yl]-propionic acid was obtained from Taiho Pharmaceutical Inc. Co. (Tokyo, Japan). Twice-daily administration was given within 1 h after meals with about 12-h intervals between doses. TSU-68 was taken for 28 consecutive days and was continued in case of stable disease or disease remission after this period for as long as no disease progression and/or no unacceptable drug-related toxicity were seen. TSU-68 administration was immediately interrupted upon the occurrence of DLT.

#### Response assessment

The objective response was assessed using the Response Evaluation Criteria in Solid Tumors (RECIST). Naïve untreated lesions were selected as targets for evaluation. At the end of each cycle, a three-phase computed tomography protocol consisting of early arterial, late arterial and portal venous phases was performed, obtaining contiguous transverse sections with a thickness of 5–7 mm. Responses were assessed independently.

#### Pharmacokinetics

In phase I, blood samples were collected from a total of 12 patients at 0 (pre-dose), 1, 2, 3, 4, 6 and 9 h post-dose on days 1 and 2 of cycle 1 and at pre-dose on day 1 of cycle 2. The plasma TSU-68 concentration was determined using high-performance liquid chromatography (HPLC). Briefly, an aliquot of plasma was mixed with acetate buffer and methanol including an internal standard. After centrifugation, the supernatant was mixed with ammonium acetate and applied to a Zorbax Eclipse XDB C18 column (3.5  $\mu$ m, 3 cm  $\times$  4.6 mm; Agilent Technologies, Mississauga, ON, Canada) of a Waters Alliance 2690 HPLC

system (Waters, Milford, MA, USA), and the effluent was monitored at 440 nm. The lower limit of quantification was 0.1 µg/ml. Non-compartmental PK parameters, including AUC,  $C_{max}$ , time to maximum concentration ( $T_{max}$ ) and elimination half-life ( $T_{1/2}$ ), were calculated using PhAST (version 2.3; MDS Pharma Services, Montreal, Quebec, Canada).

#### Angiogenesis-related markers

Blood samples were collected at baseline and at day 28 of cycle 1. The following were measured; platelet-derived growth factor (PDGF)-BB, basic fibroblast growth factor (bFGF), soluble vascular cell adhesion molecule-1 (sVCAM-1), soluble endothelial-leukocyte adhesion molecule-1 (sELAM-1) in serum and vascular endothelial growth factor-A (VEGF-A) in plasma were analyzed using enzyme-linked immunosorbent assays (ELISAs; R&D Systems, Minneapolis, MN, USA); plasma interleukin-8 (IL-8), with ELISA (BioSource Europe, Nivelles, Belgium); plasma tissue plasminogen activator (t-PA), with a soluble t-PA ELISA kit (Oncogene Science, Cambridge, MA, USA); plasma plasminogen activator inhibitor-1 (PAI-1), with a latex photometric immunoassay (LPIA; LPIA t-PAI test, Mitsubishi Kagaku Iatron, Tokyo, Japan); and plasma factor VIII, with Pathromtin SL (Dade Behring, Marburg, Germany).

#### Statistical analysis

The primary endpoint of phase I was to evaluate the safety and PK, whereas the primary endpoint of phase II was to determine the best overall response rate based on RECIST. Secondary endpoints of both phases were to evaluate the tumor necrotic effect and the relationship between blood angiogenesis-related molecules and clinical effects. We adopted the 3 + 3 study design generally used in phase I dose-escalation studies [16]. Patients were accrued using Fleming's method [17]. The target number of patients was 35, with an interim evaluation planned for the first 15 patients. The statistical power was 86% with an expected response rate of 20%, and the lower margin of efficacy and one-sided  $\alpha$ -level were both 5%. Time to progression (TTP) was defined as the interval between the first day of treatment and tumor progression or death due to any cause. Overall survival (OS) was calculated from the first day of treatment to death. TTP and OS were calculated using the Kaplan–Meier method.

The basal level of angiogenesis-related parameters to predict the response was evaluated by receiver operating characteristic (ROC) analysis. The optimal cut-off value for differentiation of responders and non-responders was defined by the point of the ROC curve (Youden index

method). After ROC analysis, logistic regression analysis was performed. The *t* test was used to compare baseline levels of angiogenesis-related parameters in term of responders.

This study is registered at ClinicalTrials.gov, number NCT 00784290.

The data were analyzed using SAS version 8.1 (SAS Institute, Cary, NC, USA).

## Results

#### Patient characteristics

From September 2003 through February 2007, 35 patients were enrolled at the University of Tokyo Hospital, Mitsui Memorial Hospital and the National Cancer Centre, all located in Tokyo, Japan. Baseline demographics and disease characteristics are summarized in Table 1. Phase I consisted of 12 patients: three patients each at Level 1 (no cirrhosis) and Level 2 (Child–Pugh A), and six patients at Level 3 (Child–Pugh B). The other 23 patients were enrolled in phase II.

In the overall study population, 29 (82.9%) of 35 patients were HCV-positive, and four (11.4%) were HBV-positive. For liver function, three (8.6%) of 35 patients were non-cirrhotic; 24 (68.6%) had Child–Pugh A cirrhosis; and eight (22.9%) had Child–Pugh B cirrhosis. Extrahepatic metastasis was found in 19 (54.3%) patients. Table 1 shows the disease stages according to the TNM classification [18, 19]: 20 (57.1%) patients were stage C (advanced), and 15 (42.9%) patients were stage B (intermediate) according to the Barcelona Clinic Liver Cancer (BCLC) Staging System [2, 20]. The patients had been treated previously a mean of 8.2 (range, 1–20) times using various modalities, including surgery, RFA and TACE. No patients ever received Sorafenib.

#### Safety and pharmacokinetics

The toxicity of TSU-68 was assessed using NCI-CTC (version 2.0) in 12 patients enrolled in phase I (Table 2). Since no DLT was found with 400 mg bid at Level 1 (no cirrhosis) or Level 2 (Child–Pugh A), the same dosage was used in Level 3 (Child–Pugh B) patients (Fig. 1a). However, patients at Level 3 on 400 mg bid experienced DLT (grade 3 abdominal pain and ascites); the dose was reduced by half, to 200 mg bid, in an additional three patients at Level 3, among whom DLT was not observed. The most common drug-related adverse events observed in phase I were hypoalbuminemia, diarrhea, abdominal pain, fever and AST/ALT elevation.

**Table 1** Patient characteristics

	Phase I		Phase II	All
	400 mg bid	200 mg bid	200 mg bid	
No. of patients	9	3	23	35
Gender				
Male	8	2	19	29
Female	1	1	4	6
Age, years				
Median	66	73	69	68
Mean	66.0	68.7	65.2	65.7
Range	53–74	60–73	49–74	49–74
ECOG performance status				
0	6	3	21	30
1	3	0	2	5
Viral markers				
HBs Ag <sup>+</sup> , HCV Ab <sup>-</sup>	2	0	2	4
HBs Ag <sup>-</sup> , HCV Ab <sup>+</sup>	6	3	20	29
HBs Ag <sup>-</sup> , HCV Ab <sup>-</sup>	1	0	1	2
Child–Pugh status				
Chronic hepatitis	3	0	0	3
A (5/6) <sup>a</sup>	3 (3/0)	0	21 (15/6)	24 (18/6)
B (7/8/9) <sup>a</sup>	3 (2/1/0)	3 (3/0/0)	2 (2/0/0)	8 (7/1/0)
Prior treatments <sup>b</sup>				
Median	8	4	9	8
Mean	8.9	6.0	8.2	8.2
Range	5–16	3–11	1–20	1–20
Disease stage <sup>c</sup>				
II	2	1	3	6
III	3	1	5	9
IVa	0	0	1	1
IVb	4	1	14	19
Extrahepatic metastasis				
Yes	4	1	14	19
No	5	2	9	16
Portal vein thrombosis				
Yes	0	0	1	1
No	9	3	22	34

<sup>a</sup> Child–Pugh score (points)

<sup>b</sup> Number of pre-treatments with surgery, radio-frequency ablation, transcatheter arterial chemoembolization, chemotherapy or radiotherapy

<sup>c</sup> Stage is based on the TNM classification [18, 19]

The PK levels were examined in nine patients (3 each at Levels 1–3) receiving 400 mg bid and in three patients (Level 3) receiving 200 mg bid, after the first dose (day 1) and the third dose (day 2; Table 3). The  $C_{\max}$  and  $AUC_{0-9h}$  did not increase with poorer liver function. In all patients, the  $C_{\max}$  and  $AUC_{0-9h}$  on day 2 were lower than those on

day 1. In Level 3, in which both 200 and 400 mg TSU-68 were evaluated, no appreciable difference in the exposure was observed on day 2 between the two dose levels. TSU-68 had not accumulated at any level when measured immediately before administration on day 29 (data not shown).

Table 2 shows all of the drug-related adverse events reported in  $\geq 10\%$  of the patients. The most common adverse events, regardless of grade, were hypoalbuminemia (57%), diarrhea (37%), anorexia (34%), abdominal pain (31%), malaise (29%), edema (29%), AST/ALT elevation (29%) and fever (23%); most were grade 1 or 2. Four patients (11.4%) experienced grade 3 or higher toxicity, and the most common grade 3–4 adverse event was AST/ALT elevation (14%). Reducing the dose of TSU-68 from 400 to 200 mg bid decreased the incidence of diarrhea, abdominal pain, fever and hypoalbuminemia. TSU-68 administration was discontinued in one patient because of anemia. However, this patient was later diagnosed with bleeding from the peritoneal dissemination of HCC invading into the colon. Most adverse events were mild, and TSU-68 was well tolerated at the dose of 200 mg bid.

#### Efficacy and survival

The antitumor effect of TSU-68 was assessed independently in the 35 patients using RECIST (Table 4). One patient at 200 mg bid achieved a complete response (CR; Fig. 2, patient 1), two patients at 200 mg bid had a partial response (PR), 15 patients had stable disease (SD), and 16 patients had progressive disease (PD). The response rate (CR + PR) was 8.6%, and the disease control rate (CR + PR + SD) was 51.4%. Disease control was maintained for >6 months in six patients. One patient did not complete the first cycle and was not evaluated (NE).

Tumor necrosis (TN) was confirmed by independent radiologists in nine patients (25.7%). Figure 2 (patient 2) is an example in which the lack of contrast enhancement and marked central hypoattenuation within the metastatic masses were consistent with TN. The magnitude of necrosis in nine patients was quantified with bi-dimensional measurements of target lesions (RECIST). The baseline mean TN was 0%, and the follow-up mean TN was 35% (5–71%). In the overall study population of 35 patients, the median TTP was 2.1 months (95% confidence interval, 1.2–2.9 months; Fig. 3a), and the median OS was 13.1 months (95% confidence interval, 6.9–26.6 months; Fig. 3b).

#### Angiogenesis-related markers

Multiple logistic regression analysis was performed. Independent variables were the data for VEGF, t-PA, sVCAM-

**Table 2** Drug-related adverse events and laboratory abnormalities by grade occurring in at least 10% of patients ( $n = 35$ )

Adverse event	Phase I ( $n = 12$ )								Phase II ( $n = 23$ )			All ( $n = 35$ )					
	Level 1 ( $n = 3$ ) 400 mg bid		Level 2 ( $n = 3$ ) 400 mg bid		Level 3 ( $n = 3$ ) 400 mg bid		Level 3 ( $n = 3$ ) 200 mg bid		200 mg bid								
	All	3	All	3	All	3	All	3	All	3	4	All	3	4			
No.	No.	No.	No.	No.	No.	No.	No.	No.	No.	No.	No.	%	No.	%	No.	%	
<b>Treatment-related adverse events</b>																	
Diarrhea	2		2		2		2		5			13	37				
Anorexia					2				10			12	34				
Abdominal pain	2				3	1	1		5			11	31	1	3		
Malaise	2								8			10	29				
Edema					1		1		8			10	29				
Fever	1		1		2				4			8	23				
Ascites					2	1	1		3			6	17	1	3		
Nausea					1				4			5	14				
Abdominal distension									4			4	11				
<b>Laboratory abnormalities</b>																	
Albumin decrease	2		3		3		1		11			20	57				
AST increase	1						2	1	7	4		10	29	5	14		
ALT increase	1						2	1	7	4		10	29	5	14		
Total bilirubin increase					1		1		6			8	23				
Alkaline phosphatase increase									7	1		7	20	1	3		
Erythropenia									7			7	20				
Hematocrit decrease	1				1				4	1		6	17	1	3		
Hemoglobin decrease	1				1				4	1	1	6	17	1	3	1	3
LDH decrease	1								5			6	17				
Thrombocytopenia	1								4	2		5	14	2	6		

Results are expressed as the worst adverse event possibly related to TSU-68 per patient based on the NCI-CTC version 2.0

**Table 3** Pharmacokinetic parameters of TSU-68 corresponding to liver function levels (mean  $\pm$  SD)

Hepatic function level ( $n = 3$ )	Dosing	$T_{max}$ (h)	$C_{max}$ ( $\mu\text{g/mL}$ )	$AUC_{0-9h}$ ( $\mu\text{g}\cdot\text{h/mL}$ )	$T_{1/2}$ (h)
Level 1 (400 mg bid)	Day 1 (1st)	3.7 $\pm$ 2.1	16.8 $\pm$ 7.1	70.1 $\pm$ 28.6	2.0 <sup>a</sup>
	Day 2 (3rd)	3.0 $\pm$ 1.0	9.5 $\pm$ 1.8	44.4 $\pm$ 11.9	2.5 $\pm$ 0.8
Level 2 (400 mg bid)	Day 1 (1st)	4.7 $\pm$ 1.2	11.7 $\pm$ 2.5	60.6 $\pm$ 19.0	2.6 <sup>a</sup>
	Day 2 (3rd)	4.0 $\pm$ 0.0	7.8 $\pm$ 1.4	36.7 $\pm$ 7.7	2.2 $\pm$ 0.9
Level 3 (400 mg bid)	Day 1 (1st)	4.0 $\pm$ 2.0	8.6 $\pm$ 4.1	46.4 $\pm$ 20.6	2.8 <sup>a</sup>
	Day 2 (3rd)	3.7 $\pm$ 0.6	5.1 $\pm$ 1.6	26.0 $\pm$ 6.9	3.0 $\pm$ 1.4
Level 3 (200 mg bid)	Day 1 (1st)	4.0 $\pm$ 0.0	5.1 $\pm$ 1.6	28.9 $\pm$ 5.2	8.2 <sup>a</sup>
	Day 2 (3rd)	3.7 $\pm$ 2.5	4.3 $\pm$ 1.4	20.7 $\pm$ 4.0	6.9 <sup>a</sup>

$AUC_{0-9h}$ , area under the concentration versus time curve for 0–9 h

<sup>a</sup>  $n = 2$

1, PAI-1, sELAM-1, IL-8, PDGF, bFGF and plasma factor VIII levels, and dependent variables were the two groups based on each cut-off level (0, below the cut-off value or 1, above the cut-off value). By logistic regression analysis,

we found that the sVCAM-1 level was an independent factor ( $P = 0.014$ ; Table 5), and sVCAM-1 (odds ratio 16.0) had the strongest influence on responders (patients with CR + PR + SD). None of the rest of the

**Table 4** Tumor response

Best response	Phase I (n = 12)		Phase II (n = 23)	Total (n = 35)	
	400 mg bid (n = 9) No.	200 mg bid (n = 3) No.	200 mg bid No.	No.	%
Complete response	0	0	1	1	2.9
Partial response	0	0	2	2	5.7
Stable disease	2	2	11	15	42.8
Progressive disease	6	1	9	16	45.7
Not evaluated <sup>a</sup>	1	0	0	1	2.9

<sup>a</sup> This patient did not complete cycle 1

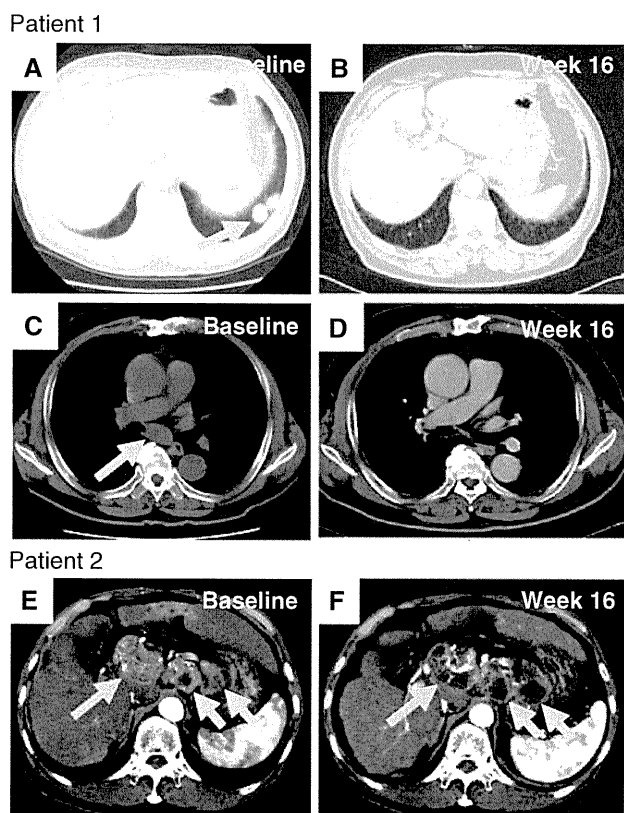


**Fig. 2** Computed tomography images of responding lesions from patient 1, who achieved a complete response. Metastatic lesions in the lung (a) and lymph node (c) disappeared after four cycles (16 weeks) of TSU-68 treatment (b, d). Representative computed tomography images of a tumor showing necrosis in patient 2. Before treatment, several abdominal lymph node metastases were apparent (e). After four cycles of treatment (16 weeks), the lesions demonstrated a lack of enhancement and markedly lower attenuation, consistent with tumor necrosis (f)

angiogenesis-related parameters showed any variation with treatment (as the variation of the data for PAI-1 was so large, they were not analyzed; Table 5). The mean values of sVCAM-1 for responders (patients with CR + PR + SD; 1,944 pg/ml) were higher than that for non-responders (patients with PD + NE; 1,422 pg/ml), which was statistically significant ( $P = 0.026$ ,  $t$  test).

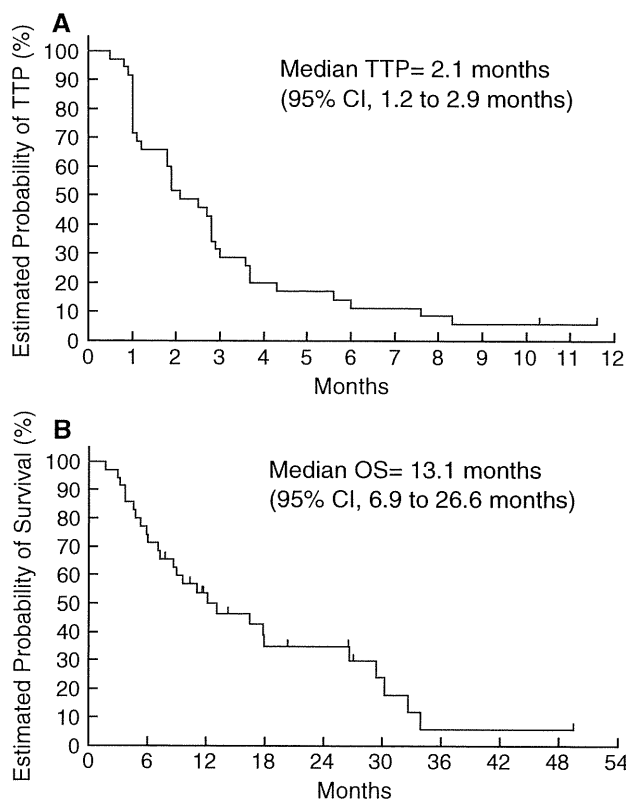


**Fig. 3** a The independently assessed median time to progression in all 35 patients treated with TSU-68 was 2.1 months. b The investigator-assessed median overall survival in all 35 patients treated with TSU-68 was 13.1 months

**Discussion**

In this trial, special attention was paid to patients with HCC, who often have impaired liver function and might have the potential for reduced clearance of TSU-68, which is eliminated mainly by the liver [12, 13]. This study suggests that the adverse-event profile of TSU-68 in this trial was comparable to observations in other phase I trials examining patients with solid tumors [14, 15]. Although half of the patients experienced exacerbation of pre-existing hypoalbuminemia during the treatment, this was

**Table 5** Logistic regression analysis of angiogenesis-related factors

Variable	Evaluation variable (cut-off point)	Odds ratio	95% CI	<i>P</i> value
VEGF	<47 × ≥47	0.480	0.095–2.426	0.375
t-PA	<2.3 × ≥2.3	2.250	0.574–8.824	0.245
VCAM-1	<2,370 × ≥2,370	16.000	1.735–147.541	0.014
ELAM-1	<70 × ≥70	0.716	0.187–2.744	0.626
IL-8	<10.0 × ≥10.0	3.250	0.761–13.889	0.112
PDGF	<1,450 × ≥1,450	3.666	0.907–14.813	0.068
Factor VIII	<181 × ≥181	0.545	0.140–2.120	0.382

The *t* test was used to compare baseline levels of angiogenesis-related parameters in terms of responders. A responder means a patient who showed CR, PR and SD; non-responders showed PD and NE

not associated with a worsening of liver function. The edema, associated with hypoalbuminemia, was managed with diuretics. The lack of hypertension as a toxic effect may have been due to the difference in the inhibitory profile between TSU-68, which strongly inhibits both PDGFR and VEGFR, and other antiangiogenic compounds, which predominantly inhibit VEGFR [21, 22].

From the viewpoint of the pharmacokinetics of TSU-68, no trend was seen toward higher plasma exposure to TSU-68 with greater liver dysfunction (Levels 1–3). Furthermore, the exposure in the patients with HCC appeared to be similar to that in patients with advanced solid tumors that were not HCC in a phase I study [15]. These findings suggest that impaired liver function is unlikely to affect the pharmacokinetics of TSU-68. The present study indicated that the  $C_{\max}$  and AUC were reduced by the repeated administration of TSU-68, which has also been observed in previous trials [14, 15]. This decrease was found to be due to TSU-68, which caused an induction of its own metabolism in the non-clinical studies [12, 13]. Although in this study, the pharmacokinetics of TSU-68 was not examined after long-term consecutive oral administration, the AUC on day 28 has been reported to be similar to that on day 2. This suggests that the decreased exposure, which reaches steady state on day 2, is maintained throughout the therapeutic cycle. In Level 3, no obvious decrease in the AUC on day 2 was observed by reducing the dose of TSU-68 from 200 to 400 mg, although these results are based on a small amount of data. In addition, the estimated daily AUC in the patients who received 200 mg TSU-68 bid was roughly similar to the AUC data showing a 50% inhibition of human xenograft tumor growth in mice (data not shown). However, these data should be interpreted cautiously because the majority of the patients who were included as Child-Pugh B had Child-Pugh scores of 7.

In this study, we selected the fixed-dose for both Child-Pugh A and B because hepatitis or Child-Pugh A patients experienced toxicities (abdominal pain and diarrhea), although no DLT was found when 400 mg bid TSU-68 was

administered, and also because liver function may fluctuate between Child-Pugh A and B in the same patients. However, whether Child-Pugh A and B can be separated depends on the safety and PK profile of the drug. Patients with Child-Pugh A are initially recommended for clinical trials in HCC research [23], whereas the design of trials that include Child-Pugh B patients needs further investigation. In addition, whether Child-Pugh score is a good system for stratifying liver function with these types of drugs is open to argument.

Many agents targeting angiogenesis have been investigated in HCC [3, 4, 10, 11, 22, 24–27]. In an international phase III trial, sorafenib reduced the mortality hazard by 44% compared with placebo, with a median OS of 10.7 months (vs. 7.9 months with placebo) [3]. In an Asian phase III trial, patients who received sorafenib had a 35% disease control rate (vs. 16% with placebo), with a median TTP of 2.8 months (vs. 1.4 months) and a median OS of 6.5 months (vs. 4.2 months) [4]. The results mirrored those of the SHARP trial, although the Asia-Pacific patients had more advanced disease. In a phase I trial in Japan, sorafenib resulted in 4% PR and 83% SD, with a median TTP of 4.9 months and a median OS of 15.6 months [24]. Sunitinib, an inhibitor of VEGFR, PDGFR and c-Kit, was used against HCC in a phase II trial and produced a 3.9% PR and 38.5% SD, with a median progression-free survival of 3.9 months and a median OS of 9.8 months [22, 25]. Chemotherapy-naïve Child-Pugh A patients were enrolled in the sorafenib phase III trial [3, 4]. In our trial, eight Child-Pugh B patients were enrolled, and systemic chemotherapy had been already administered in 14 patients. The patients had been treated previously a mean of 8.2 times using various modalities. Although TTP in our trial is less than the reported data of SHARP [3] and similar to the Asian sorafenib trial in the placebo arms [4], these factors might affect the results.

The response rate (8.6%) and a median OS (13.1 months) of TSU-68 were comparable to those reported for these other agents. Some patients were

administered TSU-68 for more than 1 year after confirmed PD by independent review that was not determined by investigators, and the long-term treatment with TSU-68 might have contributed to the longer OS period. This warrants further study, but needs to be evaluated in a larger trial. Molecular-targeted agents, including TSU-68, generally show a relatively low response rate but a high disease control rate, indicating that a large proportion of patients reach SD. The treatment response assessed using RECIST may not accurately reflect the overall effect of these agents [23]. We had several cases in which necrosis was observed inside a tumor, despite the increase in tumor size. As an objective response is a weak surrogate of activity in phase II trials, a consensus conference endorsed by the American Association for the Study of Liver Diseases and the European Association for the Study of the Liver recommended the inclusion of TTP as the primary endpoint in phase II trials [23].

Molecular-targeted agents are being developed as systemic therapies for HCC in first- and second-line settings as monotherapy and in combination with locoregional therapies. The primary endpoint for phase III studies that assess primary HCC treatments is survival, and the control arm should be sorafenib. Comparison of single agents head to head with sorafenib might jeopardize study approval and the recruitment of patients for ethical reasons. For second-line treatments against advanced HCC, the new agents should be compared with placebo or best supportive care [23]. A phase II randomized study of TSU-68 in combination with TACE has been conducted (manuscript in preparation), and a phase III trial is being planned.

VEGF, PDGF and bFGF participate in the neovascularization of HCC [26, 27], and VEGF levels are thought to have a prognostic value [28]. IL-8 has proangiogenic activity in cancers, although its role in HCC is controversial [27]. Given that the primary target of TSU-68 is endothelial cells, we speculated that damaged vascular endothelial cells may release endothelial cell-specific markers such as sELAM-1 and sVCAM-1. As sVCAM-1 can be identified in the bloodstream, it is potentially useful as a non-invasive biomarker for the monitoring of disease progression in cancer [29]. A high level of VCAM-1 was significantly associated with an advanced disease stage and the presence of distant metastasis in gastric cancer [30] and also has been shown to be associated with angiogenesis and poor prognosis in breast cancer [31] and in HCC [32]. In this trial, we found higher baseline levels of sVCAM-1 in patients with good response (CR + PR + SD) after treatment with TSU-68. Although our data suggested that sVCAM-1 is a possible predictive marker for the response, the analysis is exploratory, and further study is necessary to confirm this possibility.

In conclusion, the step-wise study design based on hepatic function was useful in a safety assessment of TSU-68 in patients with HCC who had impaired liver function. The TSU-68 dosage of 200 mg bid has a favorable safety profile, even in patients with Child–Pugh B cirrhosis, and together with a high disease control rate, provides a rationale for its further evaluation in patients with HCC.

**Acknowledgments** We thank Tomonori Fujishima, Hideo Yoshida, Miwa Yamashita, Megumi Kawai and Atsuko Tamori for their contributions. We are also grateful to Yutaka Ariyoshi, Nagahiro Saijo and Yuh Sakata for their extramural review. This study was supported by Taiho Pharmaceutical.

**Conflict of interest statement** The author(s) have nothing to disclose.

## References

1. Parkin DM, Bray F, Ferlay J et al (2005) Global cancer statistics, 2002. *CA Cancer J Clin* 55:74–108
2. Bruix J, Sherman M (2005) Management of hepatocellular carcinoma. *Hepatology* 42:1208–1236
3. Llovet JM, Ricci S, Mazzaferro V et al (2008) Sorafenib in advanced hepatocellular carcinoma. *N Engl J Med* 359:378–390
4. Cheng AL, Kang YK, Chen Z et al (2009) Efficacy and safety of sorafenib in patients in the Asia-Pacific region with advanced hepatocellular carcinoma: a phase III randomised, double-blind, placebo-controlled trial. *Lancet Oncol* 10:25–34
5. Laird AD, Vajkoczy P, Shawver LK et al (2000) SU6668 is a potent antiangiogenic and antitumor agent that induces regression of established tumors. *Cancer Res* 60:4152–4160
6. Naumova E, Ubezio P, Garofalo A et al (2006) The vascular targeting property of paclitaxel is enhanced by SU6668, a receptor tyrosine kinase inhibitor, causing apoptosis of endothelial cells and inhibition of angiogenesis. *Clin Cancer Res* 12:1839–1849
7. Yorozuya K, Kubota T, Watanabe M et al (2005) TSU-68 (SU6668) inhibits local tumor growth and liver metastasis of human colon cancer xenografts via anti-angiogenesis. *Oncol Rep* 14:677–682
8. Solorzano CC, Jung YD, Bucana CD et al (2001) In vivo intracellular signaling as a marker of antiangiogenic activity. *Cancer Res* 61:7048–7051
9. Kuenen BC, Giaccone G, Ruijter R et al (2005) Dose-finding study of the multitargeted tyrosine kinase inhibitor SU6668 in patients with advanced malignancies. *Clin Cancer Res* 11:6240–6246
10. Kanai F, Yoshida H, Teratani T et al (2006) New feasibility study design with hepatocellular carcinoma: a phase I/II study of TSU-68, an oral angiogenesis inhibitor [Abstract]. *J Clin Oncol* 24(Suppl):213S
11. Kanai F, Yoshida H, Tateishi R et al (2008) Final results of a phase I/II trial of the oral anti-angiogenesis inhibitor TSU-68 in patients with advanced hepatocellular carcinoma [Abstract]. *J Clin Oncol* 26(Suppl):235S
12. Kitamura R, Yamamoto Y, Nagayama S et al (2007) Decrease in plasma concentrations of antiangiogenic agent TSU-68 ((Z)-5-[[1, 2-dihydro-2-oxo-3H-indol-3-ylidene)methyl]-2, 4-dimethyl-1H-pyrrole-3-propanoic acid) during oral administration twice a day to rats. *Drug Metab Dispos* 35:1611–1616

13. Kitamura R, Asanoma H, Nagayama S et al (2008) Identification of human liver cytochrome P450 isoforms involved in autoinduced metabolism of the antiangiogenic agent (Z)-5-[(1, 2-dihydro-2-oxo-3H-indol-3-ylidene)methyl]-2, 4-dimethyl-1H-pyrrole-3-propanoic acid (TSU-68). *Drug Metab Dispos* 36:1003–1009
14. Ueda Y, Shimoyama T, Murakami H et al (2010) Phase I and pharmacokinetic study of TSU-68, a novel multiple receptor tyrosine kinase inhibitor, by twice daily oral administration between meals with solid tumors (under submission)
15. Murakami H, Ueda Y, Shimoyama T et al. (2010) Phase I, pharmacokinetic, and biological studies of TSU-68, a novel multiple tyrosine kinase inhibitor, administered after meals with solid tumors (under submission)
16. Green H, Benedetti J, Crowley J (2002) *Clinical trials in oncology*, 2nd edn. Chapman & Hall, London
17. Fleming TR (1982) One-sample multiple testing procedures for phase II clinical trials. *Biometrics* 38:143–151
18. The Liver Cancer Study Group of Japan (2000) The general rules for the clinical and pathological study of primary liver cancer. Version 4. Kanehara & Co., Ltd., Tokyo
19. Makuuchi M, Belghiti J, Belli G et al (2003) IHPA concordant classification of primary liver cancer: working group report. *J Hepatobiliary Pancreat Surg* 10:26–30
20. Llovet JM, Bruix J (2008) Novel advancements in the management of hepatocellular carcinoma 2008. *J Hepatol* 48:S20–S37
21. Roodhart JM, Langenberg MH, Witteveen E et al (2008) The molecular basis of class side effects due to treatment with inhibitors of VEGF/VEGFR pathway. *Curr Clin Pharmacol* 3:132–143
22. Faivre S, Raymond E, Boucher E et al (2009) Safety and efficacy of sunitinib in patients with advanced hepatocellular carcinoma: an open-label, multicentre, phase II study. *Lancet Oncol* 10:794–800
23. Llovet JM, Di Bisceglie AM, Bruix J et al (2008) Panel of experts in HCC-design clinical trials. Design and endpoints of clinical trials in hepatocellular carcinoma. *J Natl Cancer Inst* 100:698–711
24. Furuse J, Ishii H, Nakachi K et al (2008) Phase I study of sorafenib in Japanese patients with hepatocellular carcinoma. *Cancer Sci* 99:159–165
25. Zhu AX, Sahani DV, Duda DG et al (2009) Efficacy, safety, and potential biomarkers of sunitinib monotherapy in advanced hepatocellular carcinoma: a phase II study. *J Clin Oncol* 27:3027–3035
26. Thomas MB, Abbruzzese JL (2005) Opportunities for targeted therapies in hepatocellular carcinoma. *J Clin Oncol* 23:8093–8108
27. Pang R, Poon RT (2006) Angiogenesis and antiangiogenic therapy in hepatocellular carcinoma. *Cancer Lett* 242:151–167
28. Poon RT, Lau C, Pang R et al (2007) High serum vascular endothelial growth factor levels predict poor prognosis after radiofrequency ablation of hepatocellular carcinoma: importance of tumor biomarker in ablative therapies. *Ann Surg Oncol* 14:1835–1845
29. Alexiou D, Karayiannakis AJ, Syrigos KN et al (2001) Serum levels of E-selectin, ICAM-1, and VCAM-1 in colorectal cancer patients: correlations with clinicopathological features, patient survival and tumor surgery. *Eur J Cancer* 37:2392–2397
30. Alexiou D, Karayiannakis AJ, Syrigos KN et al (2003) Clinical significance of serum levels of E-selectin, intracellular adhesion molecule-1, and vascular cell adhesion molecule-1 in gastric cancer patients. *Am J Gastroenterol* 98:478–485
31. O'Hanlon DM, Fitzsimons H, Lynch J et al (2002) Soluble adhesion molecule (E-selectin, ICAM-1 and VCAM-1) in breast carcinoma. *Eur J Cancer* 38:2252–2257
32. Joanna WH, Ronnie TP, Cindy ST et al (2004) Clinical significance of serum vascular cell adhesion molecule-1 levels in patients with hepatocellular carcinoma. *World J Gastroenterol* 10:2014–2018

## High-resolution characterization of a hepatocellular carcinoma genome

Yasushi Totoki<sup>1</sup>, Kenji Tatsuno<sup>2</sup>, Shogo Yamamoto<sup>2</sup>, Yasuhito Arai<sup>1</sup>, Fumie Hosoda<sup>1</sup>, Shumpei Ishikawa<sup>3</sup>, Shuichi Tsutsumi<sup>2</sup>, Kohtaro Sonoda<sup>2</sup>, Hirohiko Totsuka<sup>4</sup>, Takuya Shirakihara<sup>1</sup>, Hiromi Sakamoto<sup>4</sup>, Linghua Wang<sup>2</sup>, Hidenori Ojima<sup>5</sup>, Kazuaki Shimada<sup>6</sup>, Tomoo Kosuge<sup>6</sup>, Takuji Okusaka<sup>7</sup>, Kazuto Kato<sup>8</sup>, Jun Kusuda<sup>9</sup>, Teruhiko Yoshida<sup>4</sup>, Hiroyuki Aburatani<sup>2</sup> & Tatsuhiro Shibata<sup>1</sup>

**Hepatocellular carcinoma, one of the most common virus-associated cancers, is the third most frequent cause of cancer-related death worldwide<sup>1</sup>. By massively parallel sequencing<sup>2</sup> of a primary hepatitis C virus–positive hepatocellular carcinoma (36× coverage) and matched lymphocytes (>28× coverage) from the same individual, we identified more than 11,000 somatic substitutions of the tumor genome that showed predominance of T>C/A>G transition and a decrease of the T>C substitution on the transcribed strand, suggesting preferential DNA repair. Gene annotation enrichment analysis<sup>3</sup> of 63 validated non-synonymous substitutions revealed enrichment of phosphoproteins. We further validated 22 chromosomal rearrangements, generating four fusion transcripts that had altered transcriptional regulation (*BCORL1-ELF4*) or promoter activity. Whole-exome sequencing<sup>4,5</sup> at a higher sequence depth (>76× coverage) revealed a *TSC1* nonsense substitution in a subpopulation of the tumor cells. This first high-resolution characterization of a virus-associated cancer genome identified previously uncharacterized mutation patterns, intra-chromosomal rearrangements and fusion genes, as well as genetic heterogeneity within the tumor.**

We sequenced short-insert (250 bp, on average) genomic libraries of a primary hepatitis C virus (HCV)–positive hepatocellular carcinoma (HCC) and lymphocytes from a Japanese male (Supplementary Fig. 1) using the Illumina GAIIX sequencer with 50-bp paired-end reads. After alignment to the human reference genome and removal of PCR duplications, we obtained high-quality nucleotide sequences covering 102.5 Gb of the tumor genome (35.9× coverage) and 80.2 Gb (28.1× coverage) of the lymphocyte genome (Supplementary Table 1). The sequenced reads covered 99.69% (tumor) and 99.79% (lymphocyte)

of the human reference genome. We identified 3,023,587 germline variations in the lymphocyte genome, approximately 90% of which were found in the dbSNP database, and 2,939,032 nucleotide variations in the tumor genome (a proportion of the variation was lost as a result of chromosomal alterations in the tumor genome). Comparison of the tumor and lymphocyte genomes revealed 11,731 somatically acquired nucleotide changes in the tumor genome (Table 1).

The prevalence of somatic substitutions was significantly less in the genic (intronic, non-coding exon and coding exon) regions relative to the intergenic regions (Fig. 1a, left), which could be partially explained by negative selection of lethal mutations in the gene regions or by the existence of specific molecules responsible for the repair of transcribed regions<sup>6</sup>. There was no significant difference in the prevalence of somatic substitutions between those of non-coding and coding exons (Fig. 1a, left), whereas the prevalence of germline variation was significantly decreased in the coding exons (Fig. 1a, right). Additionally, the ratio of non-synonymous to synonymous somatic substitutions (63/18 = 3.5) in the tumor genome was significantly higher than that of germline variations (9,573/10,552 = 0.91;  $P < 0.0001$ ) but was not significantly different from that expected by chance (3.36;  $P = 0.91$ ). This result suggests that an increase in negative selection of somatic substitution on the coding exons is weaker than that of germline variation. An alternative, but not mutually exclusive, explanation is that positive selection, which benefits the survival of tumor cells, partially occurs on the coding exons. The distribution of somatic substitutions revealed the dominance of T>C/A>G and C>T/G>A transitions (Fig. 1b). Sequence context preference was evident in some nucleotide substitutions. The C>T transition occurred significantly at CpG sites (15%;  $P < 0.0001$ ), whereas the T>C transition occurred frequently at ApT sites (40%;  $P < 0.0001$ ) (Supplementary Fig. 2). Only the T>C/A>G transition was significantly ( $P = 0.01$ ) lower in the coding exons relative to the intergenic

<sup>1</sup>Division of Cancer Genomics, National Cancer Center Research Institute, Chuo-ku, Tokyo, Japan. <sup>2</sup>Genome Science Division, Research Center for Advanced Science and Technology, University of Tokyo, Meguro-ku, Tokyo, Japan. <sup>3</sup>Department of Pathology, Graduate School of Medicine, University of Tokyo, Bunkyo-ku, Tokyo, Japan. <sup>4</sup>Division of Genetics, National Cancer Center Research Institute, Chuo-ku, Tokyo, Japan. <sup>5</sup>Division of Molecular Pathology, National Cancer Center Research Institute, Chuo-ku, Tokyo, Japan. <sup>6</sup>Hepatobiliary and Pancreatic Surgery Division, National Cancer Center Hospital, Chuo-ku, Tokyo, Japan. <sup>7</sup>Hepatobiliary and Pancreatic Oncology Division, National Cancer Center Hospital, Chuo-ku, Tokyo, Japan. <sup>8</sup>Institute for Research in Humanities, Graduate School of Biostudies, Institute for Integrated Cell-Material Sciences, Kyoto University, Kyoto, Japan. <sup>9</sup>National Institute of Biomedical Innovation, Ibaraki, Osaka, Japan. Correspondence should be addressed to T. Shibata (tashibat@ncc.go.jp).

Received 21 July 2010; accepted 14 March 2011; published online 17 April 2011; doi:10.1038/ng.804

**Table 1** Somatically acquired alterations in a liver cancer genome

Type of change	Number	Percentage
<b>Substitutions</b>	11,731	100.0
Coding	81	0.7
Nonsense	1	<0.1
Missense	62	0.5
Synonymous	18	0.2
Non-coding	120	1.0
UTR	83	0.7
Pseudogene	23	0.2
ncRNA	19	0.2
Intronic	4,001	34.1
Splice site	2	<0.1
Other	3,999	34.1
Intergenic	7,529	64.2
<b>Small insertions and deletions</b>	670	100.0
Coding	7	1.0
Non-coding	9	1.3
UTR	8	1.2
Pseudogene	0	0.0
ncRNA	2	0.3
Intronic	249	37.2
Splice site	0	0.0
Other	249	37.2
Intergenic	405	60.4
<b>Rearrangements</b>	22	100.0
Intrachromosomal	21	95.5
Deletions	11	50.0
Inversions	9	40.9
Tandem duplications	1	4.5
Interchromosomal	1	4.5

In 'non-coding' categories, some mutations have been classified into two subgroups. Four substitutions were classified as both UTR and non-coding RNA. One substitution was classified as both a pseudogene and non-coding RNA. One indel was classified as both UTR and non-coding RNA. UTR, untranslated region; ncRNA, non-coding RNA.

regions (Fig. 1c), and the C>T/G>A transition was more frequent in the coding exons relative to the intronic and non-coding exon regions, partly due to the higher GC content of coding exons and the higher frequency of CpG methylation. There were fewer T>C transitions on the transcribed strands than on the untranscribed strands ( $P < 0.0001$ ) (Fig. 1d), and we observed no statistically significant differences for other substitutions.

We detected 90 somatic substitutions in protein-coding regions, 81 (including 63 non-synonymous substitutions) of which were validated as somatic alterations by Sanger sequencing of both the tumor and lymphocyte genomes (Tables 1, 2 and Supplementary Fig. 3). Of the remaining nine substitutions, three could not be amplified by PCR, four could not be sequenced due to the surrounding repetitive sequences and two could not be validated, likely because they were located within highly homologous segmental duplications or processed pseudogene regions. We also found evidence for 670 small somatic insertions and deletions,

and all seven that are located in protein-coding regions were validated (Tables 1 and 2, Supplementary Fig. 13). These somatic alterations included mutations of two well-known tumor suppressor genes for HCC (*TP53* and *AXIN1*) and five genes (*ADAM22*, *JAK2*, *KHDRBS2*, *NEK8* and *TRRAP*) that have been found to be mutated in other cancers<sup>7</sup>. Gene annotation enrichment analysis<sup>3</sup> of the non-synonymous somatic mutations revealed significant overrepresentation of genes encoding phosphoproteins ( $P = 0.0017$ ) and those with bipartite nuclear localization signals ( $P = 0.029$ ) (Supplementary Table 2). Further re-sequencing of the exons containing potentially deleterious mutations in 96 additional pairs of primary HCC and non-cancerous liver and 21 HCC cell lines revealed two mutations (resulting in p.Phe190Leu and p.Gln212X, of which only the latter was proven to be somatic) in *LRRC30* (Supplementary Fig. 4). *LRRC30* contains nine repeats of a leucine-rich domain of unknown function, and all validated mutations changed the well-conserved amino acid in these repeats or produced a truncated protein.

We predicted 33 somatic rearrangements, 22 of which were validated by Sanger sequencing of the breakpoints in both the tumor and lymphocyte genomes (Table 3). Most of the rearrangements were intra-chromosomal and occurred at the boundaries of copy number change (Supplementary Fig. 5). In particular, nine structural aberrations were clustered in the region of 11q12.2–11q13.4, generating a complex pattern of chromosomal amplification and loss (Supplementary Fig. 6). RT-PCR and sequencing analysis of the tumor and matched non-cancerous liver tissue validated four somatic fusion transcripts generated by rearrangements: the *BCORL1-ELF4* and *CTNND1-STX5* fusion genes by intra-chromosomal inversions (Xq25 and 11q12, respectively), the *VCL-ADK* fusion gene by an interstitial deletion in 10q22 (Supplementary Fig. 7) and the *CABP2-LOC645332* fusion gene by a tandem duplication in 11q13 (Supplementary Fig. 8). The *BCORL1-ELF4* chimeric transcript combining exons 1–11 of *BCORL1* and exon 8 of *ELF4* encodes an in-frame fusion protein (Fig. 2a,b). Quantitative RT-PCR revealed increased (>sixfold) expression of fusion transcripts in the tumor relative to wild-type *BCORL1* and *ELF4* gene expression in the non-cancerous liver (data not shown). *BCORL1* associates with CtBP and class II histone deacetylases and functions as a transcriptional repressor<sup>8</sup>, and *ELF4* encodes a transcriptional activator<sup>9,10</sup> (Fig. 2b). We expressed *BCORL1*, *ELF4* and the chimera *BCORL1-ELF4* as Gal4-DBD fusion proteins and evaluated their transcriptional activities using a luciferase reporter assay. The chimeric protein had reduced repression activity compared to wild-type *BCORL1* (Fig. 2c). For the *CTNND1-STX5* fusion gene, the combination of non-coding exon 1 of *CTNND1* and exons 3–11 of *STX5* resulted in the deletion of 96 amino acids at the terminal end of *STX5* and increased (>twofold) *STX5* gene expression in the tumor,

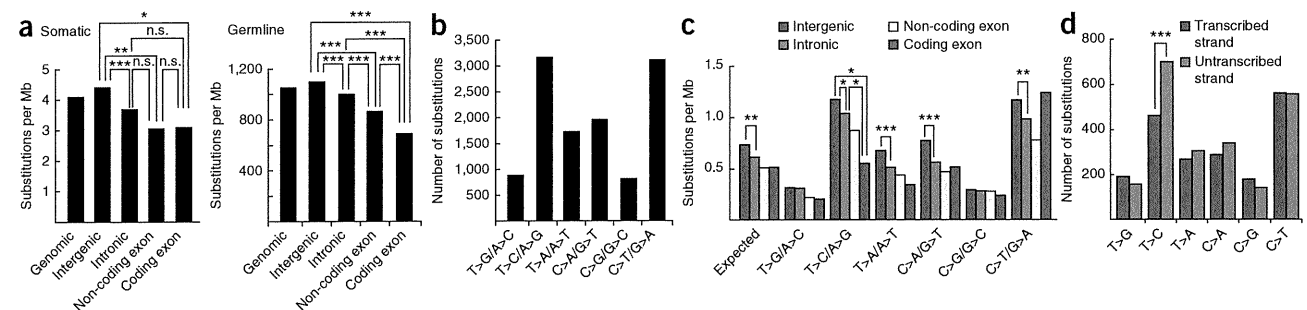


**Figure 1** Somatic substitution pattern of the liver cancer genome. (a) Prevalence of somatic and germline substitutions in different genome regions. (b) Number of each type of somatic substitution in the liver cancer genome. (c) Prevalence of each type of somatic substitution in different genome regions. (d) Number of each type of somatic substitution on the transcribed and untranscribed strands. \* $P < 0.05$ , \*\* $P < 0.01$ , \*\*\* $P < 0.0001$ .